Alzheimer's & Dementia 13 (2017) 152-167

Featured Article

mTOR and neuronal cell cycle reentry: How impaired brain insulin signaling promotes Alzheimer's disease

Andrés Norambuena[a,*], Horst Wallrabe[a], Lloyd McMahon[b], Antonia Silva[a], Eric Swanson[a], Shahzad S. Khan[a], Daniel Baerthlein[a], Erin Kodis[a], Salvatore Oddo[c], James W. Mandell[d], George S. Bloom[a,b,e,**]

[a]Department of Biology, University of Virginia, Charlottesville, VA, USA
[b]Department of Cell Biology, University of Virginia, Charlottesville, VA, USA
[c]Neurodegenerative Disease Research Center, Biodesign Institute, School of Life Sciences, Arizona State University, Tempe, AZ, USA
[d]Department of Pathology, University of Virginia, Charlottesville, VA, USA
[e]Department of Neuroscience, University of Virginia, Charlottesville, VA, USA

Abstract A major obstacle to presymptomatic diagnosis and disease-modifying therapy for Alzheimer's disease (AD) is inadequate understanding of molecular mechanisms of AD pathogenesis. For example, impaired brain insulin signaling is an AD hallmark, but whether and how it might contribute to the synaptic dysfunction and neuron death that underlie memory and cognitive impairment has been mysterious. Neuron death in AD is often caused by cell cycle reentry (CCR) mediated by amyloid-β oligomers (AβOs) and tau, the precursors of plaques and tangles. We now report that CCR results from AβO-induced activation of the protein kinase complex, mTORC1, at the plasma membrane and mTORC1-dependent tau phosphorylation, and that CCR can be prevented by insulin-stimulated activation of lysosomal mTORC1. AβOs were also shown previously to reduce neuronal insulin signaling. Our data therefore indicate that the decreased insulin signaling provoked by AβOs unleashes their toxic potential to cause neuronal CCR, and by extension, neuron death.
© 2016 the Alzheimer's Association. Published by Elsevier Inc. All rights reserved.

Keywords: Amyloid-β oligomers; Tau; Rac1; Alzheimer's disease; Cell cycle reentry; Insulin; Diabetes

1. Introduction

The most conspicuous histopathological features of Alzheimer's disease (AD) brain include two types of poorly soluble aggregates: extracellular plaques made from amyloid-β (Aβ) peptides and intraneuronal tangles assembled from the neuron-specific protein, tau. Complementing plaques and tangles as the criteria for diagnosing AD are behavioral symptoms that result from synaptic dysfunction of neurons that mediate memory and cognition and the death of those neurons [1]. Although soluble forms of Aβ and tau work coordinately to drive AD pathogenesis [2], a detailed mechanistic understanding of the normal signaling networks that go awry in AD and the pathological networks that are activated has remained an elusive goal.

Despite the limited degree to which signaling processes in AD are understood, several important clues have been recognized. One such clue concerns impaired brain insulin signaling. Glucose uptake within the brain is reduced in AD patients [3], and postmortem studies have revealed dramatically reduced expression of receptors for insulin and insulin-like growth factor 1 in the hippocampus and hypothalamus [4]. Although type 1 and type 2 diabetes are strong risk factors for AD, decreased insulin signaling in AD brain typically occurs even in patients without systemic diabetes, prompting the suggestion that AD represents brain-specific, or type 3, diabetes [3,4]. It is widely assumed that

The authors have no conflicts of interest to report.
*Corresponding author. Tel.: +1 434-982-5809; Fax: +1 434-243-3578.
**Corresponding author. Tel.: +1 434-2453-3543; Fax: +1 434-243-3578.
E-mail address: an2r@virginia.edu (A.N.), gsb4g@virginia.edu (G.S.B.)

http://dx.doi.org/10.1016/j.jalz.2016.08.015
1552-5260/© 2016 the Alzheimer's Association. Published by Elsevier Inc. All rights reserved.

diminished insulin signaling must elicit broad deleterious effects on brain metabolism, but exactly how those effects lead to synaptic dysfunction and neuron death has been puzzling.

Neuron death in brain regions affected in AD can be massive, involving loss of up to two-thirds of hippocampal CA1 neurons [5] and 90% of the neurons in selective neocortical areas [6]. The majority of these postmitotic neurons apparently die by an ironic pathway: ectopic cell cycle reentry (CCR) [7,8]. Although differentiated neurons in normal adult brain are permanently postmitotic and thereby arrested in G0, up to 10% of the neurons in regions affected by AD show signs of re-entering the cell cycle at any given time during pre-symptomatic disease stages. These cells apparently never divide, however, and their eventual disappearance from brain is matched by a commensurate loss of neurons in the same regions [9]. AD thus represents a striking contrast to cancer in the sense that AD symptoms arise in part because cells that attempt to divide die instead, whereas cancer symptoms result from cell proliferation run amok. It follows naturally that identifying proteins required for neuronal CCR and defining the relevant signaling networks hold promise for diagnosing AD at its earliest stages and developing new therapies to impede AD progression.

We recently reported the framework of a signaling network that causes CCR in AD [10]. The mechanism involves Aβ oligomer (AβO)–induced activation in parallel of three protein kinases—fyn, protein kinase A (PKA), and calcium/calmodulin-activated kinase II (CaMKII)—which then must respectively phosphorylate tau at Y18, S409, and S416. All these occur in cultured neurons within hours of initial AβO exposure and thus may be a seminal process in AD pathogenesis. We also demonstrated tau-dependent CCR in vivo by comparison of AD model mice that either expressed or lacked tau genes and confirmed prior reports [10–12] that mTOR kinase activity is required for neuronal CCR.

mTOR is a constituent of two multiprotein complexes, mTORC1 and mTORC2, that regulate fundamental cellular behavior, such as protein synthesis, cell growth, cell cycle progression, and autophagy, in response to cell surface receptors that detect insulin, growth factors, and nutrients, like amino acids. These functions require tight regulation of mTOR kinase activity at lysosomes and the plasma membrane (PM) [13,14], and mTORC1 and mTORC2 cross-regulate each other by positive and negative feedback mechanisms [15,16]. mTOR kinase activity is chronically elevated in AD brain [17], and overexpression or suppression of mTOR in AD model mice respectively aggravate or relieve AD-like pathology and behavioral deficits [18,19]. We now provide evidence for how mTOR is dysregulated by AβOs and works through tau to drive insulin-sensitive CCR, a prelude to neuron death in AD.

2. Methods

2.1. Amyloid-β oligomers

Lyophilized, synthetic $A\beta_{1–42}$ (GL Biochem, Ltd.) was dissolved in 1,1,1,3,3,3-hexafluoro-2-propanol (Sigma-Aldrich) to ~1 mM and evaporated overnight at room temperature. The dried powder was resuspended for 5 minutes at room temperature in 40–50 μL dimethylsulfoxide to ~1 mM and sonicated for 10 minutes in a water bath. To prepare oligomers, the dissolved, monomeric peptide was diluted to ~400 μL (100 μM final concentration) in Neurobasal medium (Life Technologies/Gibco), incubated 24–48 hours at 4°C with rocking and then centrifuged at 14,000 *g* for 15 minutes to remove fibrils. For all experiments with primary neurons (see Section 2.2), AβOs were diluted into tissue culture medium to a final concentration of 1.5 μM total $A\beta_{1–42}$.

2.2. Primary neurons

Primary neuron cultures were prepared from dissected brain cortices of E17/18 wild-type (WT) or tau knockout (KO) [20] mice as described previously and maintained in Neurobasal medium supplemented with B27 (Life Technologies/Gibco) [10]. Lentivirus transductions were performed at 7 days in culture, and all experiments were completed after neurons had been in culture for a total of 10–11 days. For CCR and most mTOR kinase assays, neurons were grown in B27-free Neurobasal for 5 hours before addition of AβOs. To identify neurons in S-phase, bromodeoxyuridine (BrdU; Sigma-Aldrich) was added to medium to 10 μM simultaneously with AβOs. For mTOR kinase and immunofluorescence assays shown in Figs. 2A, 5A and B, neurons were incubated in Hank balanced salt solution for 2 hours before a 30-minute exposure to AβOs, 1 μM insulin, or a mixture of 0.398 mM L-arginine plus 0.8 mM L-leucine. For Fig. 5C and Supplementary Fig. 1, neurons were incubated in B27-free Neurobasal for 2 hours before addition of insulin (to 1 μM) or amino acids (0.398 mM L-arginine plus 0.8 mM L-leucine), 10 minutes after which AβOs were added. The cells were fixed and stained for immunofluorescence or in-cell Western blot analysis [10] 24 hours later. Rapamycin, NSC23766 (both from Calbiochem) and bovine pancreatic insulin (Sigma-Aldrich, cat. no. I5500) were diluted into medium to 100 nM, 10 μM, and 500 nM, respectively. Cultures were preincubated with Torin1 (500 nM; kindly provided by Dr John Lazo, University of Virginia) 2 hours before addition of AβOs. Cell-permeable TAT peptides were purchased from GL Biochem, Ltd.

2.3. Antibodies

For primary and secondary antibodies, see Supplementary Table 1.

2.4. Complementary DNA constructs and shRNA sequences

The pEGFP-Rac1$_{WT}$ vector was a gift from Drs Martin Schwartz (Yale) and Konstadinos Moissoglu (National Institutes of Health). The pEGFP Rac1$_{C178S}$ construct was provided by Dr Miguel del Pozo (Fundación Centro Nacional de Investigaciones Cardiovasculares Carlos III, Spain). These constructs were amplified by polymerase chain reaction (PCR) and transferred to the lentiviral vector pBOB-NepX (Addgene plasmid 12,340; deposited by Dr Inder Verma, The Salk Institute) between the BamHI and HpaI sites using the following primers: forward 5′ TGC GGA TCC GCA ATG GTG AGC AAG GGC GAG 3′ and reverse 5′ CGC GTT AAC GCG TTA CAA CAG GCA TTT TCT 3′. The WT human 2N4R tau complementary DNA was described previously [10]. The human 4EBP1 WT and double-phospho null T37A/T46A were provided by Dr Jing Zhang (Johns Hopkins). These constructs were amplified by PCR and cloned into the lentiviral expression vector, pLJM1 FLAG Raptor-H-Ras25 (see subsequent vector information), between the SalI and EcoRV restriction sites by using the following primers: forward 5′ TGC GTC GAC TAT GAT ATG TCC GGG GGC A 3′ and reverse 5′ TGG CTA TAG AAT GTC CAT CTC AAA CTG 3′. An S262A human 2N4R tau vector was provided by Dr Alejandra Alonso (College of Staten Island). This construct was amplified by PCR and transferred to pBOB-NepX between the AgeI and HpaI sites using the following primers: forward 5′ TTA ACC GGT ATG GCT GAG CCC CGC CAG 3′ and reverse 5′ ATT GTT AAC CTA CAA ACC CTG CTT GGC CAG 3′. The pLJM1 FLAG-Raptor-Rheb15 and pLJM1 FLAG-Raptor-H-Ras25 lentiviral expression constructs were from Addgene (plasmids 19,312 and 26,637, respectively; both were deposited by Dr David Sabatini, Massachusetts Institute of Technology).

For small hairpin RNA (shRNA) knockdowns, the following published oligonucleotide-targeting sequences were inserted into the pLKO.1 vector (Addgene plasmid 10,878; deposited by Dr David Root, Broad Institute) following the manufacturer recommendations:

1) shNCAM = 5′ CGA CTT TGG CCA CTA TAC 3′.
2) shRac1 = 5′ G AGG AAG AGA AAA TGC CTG 3′.
3) shRalA = 5′ A AGG CAG GTT TCT GTA GAA 3′.
4) shGαs = 5′A GGC GCA GCG CGA GGC CAA 3′.
5) shTsc2 = 5′ GGT GAA GAG AGC CGT ATC 3′. Knockdown efficiencies were monitored by Western blotting.
6) Plasmids to knockdown Raptor and Rictor were purchased from Addgene (plasmids 21,339 and 21,341, respectively; both deposited by Dr David Sabatini). Knockdown efficiencies were monitored by Western blotting for 4EBP1/2$_{pT37/pT46}$.
7) Plasmid to knockdown Nprl3 was from the RNAi Consortium of the Broad Institute (TRCN0000175195). Knockdown efficiency was monitored by Western blotting.
8) The scrambled shRNA plasmid was from Addgene (Plasmid 1864; deposited by Dr David Sabatini).

2.5. Lentivirus production and infection

pBOB-NepX or pLKO.1 expression plasmids, and the packaging vectors, pSPAX2 and pMD2.G (Addgene plasmids 12,260 and 12,259, respectively, both deposited by Dr Didier Trono, École Polytechnique Fédérale de Lausanne) were transfected using Lipofectamine 2000 (Life Technologies) into HEK293T cells grown in 15 cm Petri dishes to ∼80% confluence in Dulbecco's MEM (Invitrogen) supplemented with 10% HyClone cosmic calf serum (GE Healthcare). Each transfection was with 30 μg total DNA at a 50%/37.5%/12.5% ratio of expression vector/pSPAX2/pMD2.G. Transfection medium was replaced with fresh medium after 24 hours, and lentivirus-conditioned medium was collected 48 and 72 hours after the start of transfection. Lentiviral particles were concentrated in a Beckman Coulter Optima LE-80K ultracentrifuge for 2 hours at 23,000 rpm (95,000 g_{av}) at 4°C in an SW28 rotor, resuspended in 400 μL Neurobasal medium and stored at −80°C in 20 μL aliquots. Cultured neurons were infected with a viral multiplicity of infection of 5 and incubated for 24 hours at 37°C, after which lentiviral medium was replaced with fresh Neurobasal plus B27.

2.6. Microscopy

Cultured neurons growing on #1 thickness, 12 mm round glass coverslips in 24-well dishes were rinsed in phosphate-buffered saline (PBS) and fixed for 15 minutes in 3.7% formaldehyde. Next, they were washed and permeabilized in washing buffer (0.2% Triton X-100 in PBS) three times for 5 minutes each, incubated for 60 minutes in blocking buffer (1 M glycine, 0.2% Triton X-100, 3% BSA in PBS), and transferred to PBS.

For experiments in which cell surface binding of AβOs was analyzed, all steps described previously were done in the absence of detergents. Binding of AβOs to neurons was substantial at 10 days in culture and did not significantly increase by 15 days in culture (Supplementary Fig. 1).

For BrdU uptake experiments, nuclear BrdU antigenicity was enhanced before antibody labeling by incubating neurons in the following order: 1) 10 minutes in 1 N HCl on ice; 2) 10 minutes at room temperature; 3) 20 minutes at 37°C in 2 N HCl; 4) acid neutralization with 0.1 M sodium borate pH 8.6 for 12 minutes at room temperature; and 5) transfer to PBS. Fixed neurons were incubated for 1 hour each with primary and secondary antibodies diluted into PBS containing 3% BSA, with several PBS washes after each antibody step. Finally, coverslips were mounted onto glass slides using Fluoromount-G (Southern Biotech, Inc.). Samples were imaged on a Zeiss Axiovert 100 [10] or a

Nikon Eclipse Ti equipped with a Yokogawa CSU-X1 spinning disk head, ×60 and ×100 1.4 NA Plan Apo objectives, and 405 nm, 488 nm, 561 nm, and 640 nm lasers. Colocalization of mTOR or TSC2 with LAMP1 was quantified by the Manders Coefficient plug-in (http://www.uhnresearch.ca/facilities/wcif/software/Plugins/Manders_Coefficients.html) for ImageJ (http://rsbweb.nih.gov/ij/index.html), which is based on the Pearson correlation coefficient [21].

Floating 50-μm-thick mouse brain sections were obtained from 3xTg [22], Tg2576 [23], and Tg2576 mice hemizygous for mTOR expression in brain [24]. 3xTg mice were fed mouse chow containing microencapsulated rapamycin from 2 to 18 months of age [19]. Sections were rinsed in PBS for 5 minutes and then incubated with blocking buffer (PBS plus 5% normal goat serum) for 2 hours at room temperature. Sections were incubated in suspension with primary antibodies for 16 hours at 4°C and with secondary antibodies for 2 hours at room temperature. Antibodies were diluted into PBS containing 2% normal goat serum and 0.05% Tween 20 (PBS/Tween20) and incubated with tissue sections with gentle rocking. Three 10-minute PBS/Tween20 washes followed each antibody step. After the final wash, the sections were rinsed with PBS and mounted between #1 thickness coverslips and glass slides using Fluoromount G. Sections were imaged on the Nikon Eclipse Ti or on a Leica TCS SP5 X scanning laser confocal microscope equipped with a × 63, 1.4 NA Plan Apo objective and a 488-nm argon laser line for imaging AlexaFluor 488 and a white light laser tuned to 590 nm for imaging AlexaFluor 594. For statistical analysis, at least 2000 NeuN-positive cells were counted per brain section along the cortices.

Human cortical brain biopsy samples, routinely obtained during placement of ventricular peritoneal shunt, were from 12 white, non-Hispanic patients who presented clinically with normal pressure hydrocephalus (Supplementary Fig. 7). Samples were fixed within 30 minutes of the procedure in 10% zinc formalin. All biopsy samples were archival material that remained after diagnosis, and the Institutional Review Board of the University of Virginia approved the use of these tissues for the procedures described here. After fixation, the samples were embedded in paraffin, sectioned to 4 μm thickness and mounted on glass slides. Paraffin was removed using xylenes before further processing for immunofluorescence, which was performed as described previously for mouse brain sections, except that the tissue was adsorbed to glass for all steps and primary antibody incubations were for 2 hours at room temperature. Immediately before sealing the slides to glass coverslips with Fluoromount G, lipofuscin autofluorescence was eliminated using the Autofluorescence Eliminator reagent (Millipore) after the manufacturer's protocol. Immunoperoxidase labeling was performed using the Dako Envision Flex detection reagent on a Dako Autostainer platform.

2.7. Immunoblotting

Samples were resolved by sodium dodecyl sulfate–polyacrylamide gel electrophoresis (SDS-PAGE) using 10% or 12% acrylamide/bis-acrylamide gels and transferred to 0.22 μm nitrocellulose (Bio-Rad). Membranes were blocked with Odyssey blocking buffer (LI-COR) and were incubated with primary antibodies and secondary IRDye-labeled antibodies (Supplementary Tables 2 and 3) diluted into antibody buffer (Odyssey blocking buffer diluted 1:1 in PBS/0.2% Tween 20). All antibody incubations were for 1 hour at room temperature or overnight at 4°C, and three washes of 5 minutes each with PBS/0.1% Tween 20 were performed after each antibody step. Membranes were dried between sheets of filter paper before quantitative imaging with an Odyssey imaging station (LI-COR).

2.8. In-cell Western blots

Primary neurons were cultured for 10 days as described earlier but were plated into 12-well dishes at a density of 250,000 cells per well. Neurons were incubated in B27-free Neurobasal for 2 hours before addition of insulin (to 1 μM) or amino acids (to 0.398 mM L-arginine plus 0.8 mM L-leucine), 10 minutes after which AβOs were added; 24 hours later, cells were fixed in 4% PFA for 15 minutes and then washed with PBS without detergents for 15 minutes (3×, 5 minutes each). Fixed cells were incubated at room temperature for 60 minutes with Odyssey blocking buffer (LI-COR) and then for 1 hour with primary (6E10 mouse anti-Aβ and rabbit anti-NrCAM) and infrared-labeled IRDye secondary antibodies (LI-COR) diluted into Odyssey blocking buffer. After each antibody step, the cultures were washed five times in PBS. The dishes were allowed to dry at least for 2 hours in the dark, and then were scanned using the LI-COR Odyssey imaging station according to the manufacturer's instructions, with a 3.0-mm offset and a scan intensity of 3.0. The intensity ratio for 6E10 to NrCAM was calculated and normalized to the level in untreated samples and was expressed as mean ± standard error of the mean.

2.9. Lipid raft isolation

Cultured neurons ($\sim 1 \times 10^6$ cells growing in a 10-cm petri dish) were homogenized in ice-cold TNE buffer (25 mM Tris, pH 7.5, 150 mM NaCl, 2 mM EGTA) containing 0.1% Triton X-100 (Sigma-Aldrich). Each homogenate (1 mL) was adjusted to 40% sucrose by the addition of 1 mL of 80% sucrose in TNE and placed at the bottom of an 5-mL ultracentrifuge tube. A 5%–30% discontinuous sucrose gradient (0.5 mL of 5% sucrose and 2.5 mL of 30% sucrose, both in TNE) was layered on top of the homogenate, after which the sample was spun in a Beckman Coulter TLX tabletop ultracentrifuge using a TLS-55 swinging bucket rotor at 52,000 rpm (180,000 g_{av}). Twelve fractions

of 410 μL each were collected from the top of the centrifuge tube. Lipid raft proteins partitioned into the lowest density fractions.

3. Immunoprecipitation

WT cortical neurons were transduced with lentiviruses to express either GFP-Rac1 WT or GFP-Rac1$_{C178S}$ for 72 hours. Cells were then lysed in ice-cold CHAPS (3-[(3-cholamidopropyl)dimethylammonio]-1-propanesulfonate) buffer (120 mM NaCl, 1 mM EDTA, 40 mM HEPES, pH 7.4, 50 mM NaF, 10 mM β-glycerophosphate, 0.3% CHAPS, 1 mM Na_3VO_4, 1 mM phenylmethylsulfonyl fluoride, 10 μg/mL leupeptin, 10 μg/mL aprotinin, 1 mM $MgCl_2$) for 30 minutes at 4°C. Cellular debris was cleared by centrifugation at 17,000 *g* for 10 minutes at 4°C in a bench top centrifuge. The supernatant was collected and incubated on a vertical rotator with 5 μg/mL of either anti-GFP or anti-NeuN for 2 hours at 4°C. Finally, 25 μL of protein G magnetic beads (New England Biolabs) was added to each supernatant and incubated for 1 hour at 4°C. Immunoprecipitates were washed three times with CHAPS buffer and eluted by adding SDS-PAGE sample buffer. For competitive assays with cell-permeant TAT peptides, WT cortical neurons expressing GFP-Rac1$_{WT}$ were treated with 20 μM TAT peptides for 5–6 hours and then were processed for immunoprecipitations as just described.

3.1. Statistics

The student *t* test was used for analyzing bar graphs, the tables shown in Figs. 4C and 6B, and the line graph shown in Supplementary Fig. 5D. A minimum of 150 cells per condition from a total of at least 3 experiments for all bar graphs and from 2 experiments for the tables were used. Data from three experiments were used for the line graph.

4. Results

4.1. mTORC1 and mTORC2 are required for neuronal CCR

To determine whether one or both mTOR complexes are required for CCR, we treated cultured WT mouse cortical neurons with shRNA to reduce the levels of Raptor or Rictor, which are respective defining subunits of mTORC1 and mTORC2. To measure knockdown efficiency, we used quantitative Western blotting to monitor phosphorylation of the mTORC1 substrate, 4EBP1/2 (at T37 and T46), and the mTORC2 substrate, Akt (at S473). To monitor CCR simultaneously, we exposed AβO-treated and control untreated neurons to BrdU, a synthetic nucleotide that can covalently incorporate into DNA, and used anti-BrdU immunofluorescence microscopy to identify nuclei that had incorporated BrdU and thus had entered S-phase of the cell cycle. The cultures were also stained for immunofluorescence with antibodies to the neuron-specific proteins, MAP2 and tau, to discriminate neurons from the glial cells that were also present.

As shown in Fig. 1A, ~5% of the neurons were BrdU positive in the absence of AβOs, but the level rose to ~40% after AβO treatment. Knockdown of either Raptor or Rictor completely blocked AβO-induced BrdU incorporation by neurons. Similar results for BrdU incorporation were obtained by directly inhibiting mTORC1 with rapamycin, or both mTORC1 and mTORC2 with Torin1 (Supplementary Fig. 2). Torin1 also strongly reduced AβO-induced phosphorylation of 4EBP1/2 at T37 and T46, and of another mTORC1 substrate, p70/S6 kinase (S6K) at T389 (Fig. 1B). These collective results indicate that both mTORC1 and mTORC2 are required for AβO-stimulated neuronal CCR.

Expression of the nuclear G1 marker, cyclin D1, at a level sufficient for cell proliferation is enabled by the translation regulator, eIF4E, whose activity is inhibited by its binding to 4EBPs [25]. When 4EBPs are phosphorylated at T37 and T46 by mTORC1, however, they dissociate from eIF4E, thereby enabling cell cycle progression [25]. We found that Tg2576 AD model mice [23] with hemizygous, as compared with homozygous mTOR expression in brain [24], had an approximate 4-fold reduction in cortical neurons expressing cyclin D1 or the G1/S/G2 marker, Ki67 [26] (Fig. 1C). mTOR haploinsufficiency in Tg2576 mice rescues memory deficits [24] and dramatically reduces cortical eIF4E immunostaining (Fig. 1C), suggesting that aberrant regulation of translation through the mTOR/eIF4E pathway promotes AD.

4.2. AβOs activate mTORC1 at the PM but not at lysosomes

mTOR is thought to act primarily at lysosomes and the PM [13,14,27,28]. To determine where AβOs activate mTORC1 in cultured neurons, we forced mTORC1 to accumulate preferentially on lysosomes or the PM by lentiviral expression in cultured neurons of FLAG-Raptor fused either to a lysosome-targeting region of Rheb (FLAG-Raptor-Rheb15) or a PM-targeting region in H-Ras25 (FLAG-Raptor-H-Ras25) [29]. Quantitative Western blotting indicated that mTORC1 kinase activity, as measured by 4EBP1/2$_{pT37/pT46}$/4EBP1$_{total}$, increased approximately 2-fold after exposure of neurons expressing FLAG-Raptor-H-Ras25 to AβOs, insulin, or both. In neurons expressing FLAG-Raptor-Rheb15, mTORC1 activity rose similarly in response to insulin or insulin plus AβOs but not significantly after exposure to AβOs alone (Fig. 2A). AβOs also induced nuclear cyclin D1 accumulation in ~25% of both nontransduced neurons and neurons expressing FLAG-Raptor-H-Ras25. In contrast, nuclear cyclin D1 was not induced by AβOs in neurons expressing FLAG-Raptor-Rheb15 (Fig. 2B). Insulin thus efficiently stimulates mTORC1 at the PM and lysosomes, whereas AβOs stimulate mTORC1 only at the PM.

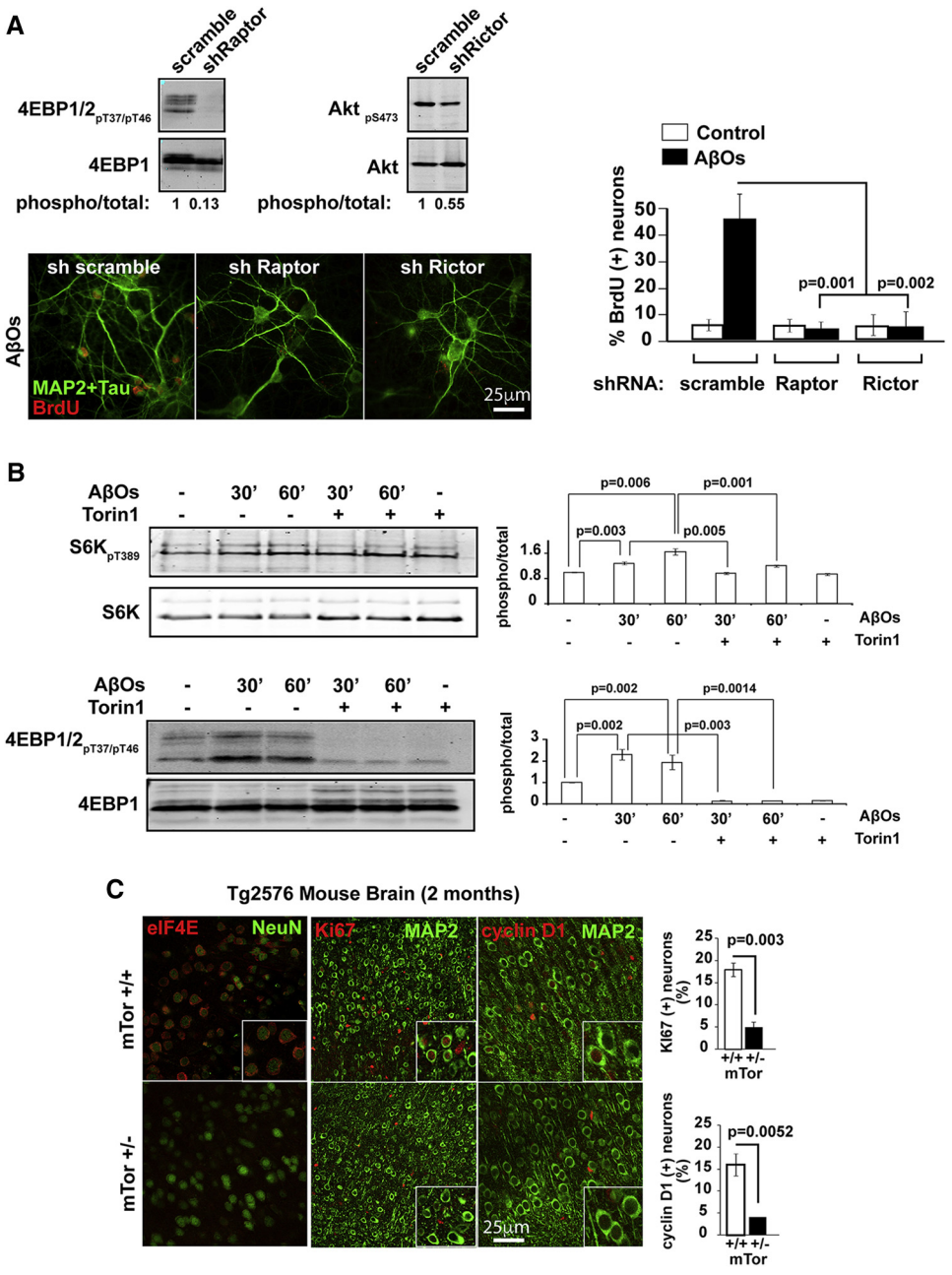

Fig. 1. mTOR is required for cell cycle reentry (CCR) in vitro and in vivo. (A) Knocking down Raptor or Rictor inhibits phosphorylation of the respective mTORC1 and mTORC2 substrates, 4EBP1/2 at T37 and T46 and Akt at S473, and blocks amyloid-β oligomer (AβO)–induced nuclear uptake of bromodeoxyuridine (BrdU). (B) Torin1 inhibits AβO-induced phosphorylation of the mTORC1 substrates, S6K (at T389) and 4EBP1/2. (C) mTOR haploinsufficiency suppresses neuronal CCR. Error bars in all panels represent standard error of the mean.

To seek further support for these observations, we also forced 4EBP1 to accumulate at the PM by expressing either FLAG-4EBP1$_{WT}$ or the nonphosphorylatable FLAG-4EBP1$_{T37A/T46A}$ mutant fused to the same PM targeting region of H-Ras-25. AβOs induced nuclear accumulation of cyclin D1 in ∼25% of control, nontransduced neurons, or neurons expressing FLAG-4EBP1$_{WT}$-H-Ras25, but <15% of neurons expressing FLAG-4EBP1$_{T37A/T46A}$-H-Ras25 were positive for nuclear cyclin D1 after AβO exposure (Fig. 2C). AβO-stimulated phosphorylation of 4EBP1 at T37 and T46 by PM-associated mTORC1 therefore promotes neuronal CCR.

To determine if the PM-specific activation of mTORC1 by AβOs requires tau, we targeted mTORC1 to the PM or lysosomes by respective lentiviral expression of FLAG-Raptor-H-Ras25 or FLAG-Raptor-Rheb15 in primary neurons derived from tau KO mice (tau KO neurons). In the absence of lentiviral expression, AβOs stimulated 4EBP1/2 phosphorylation only half as well in tau KO neurons as in WT neurons (Supplementary Fig. 3B). When FLAG-Raptor-H-Ras25 or

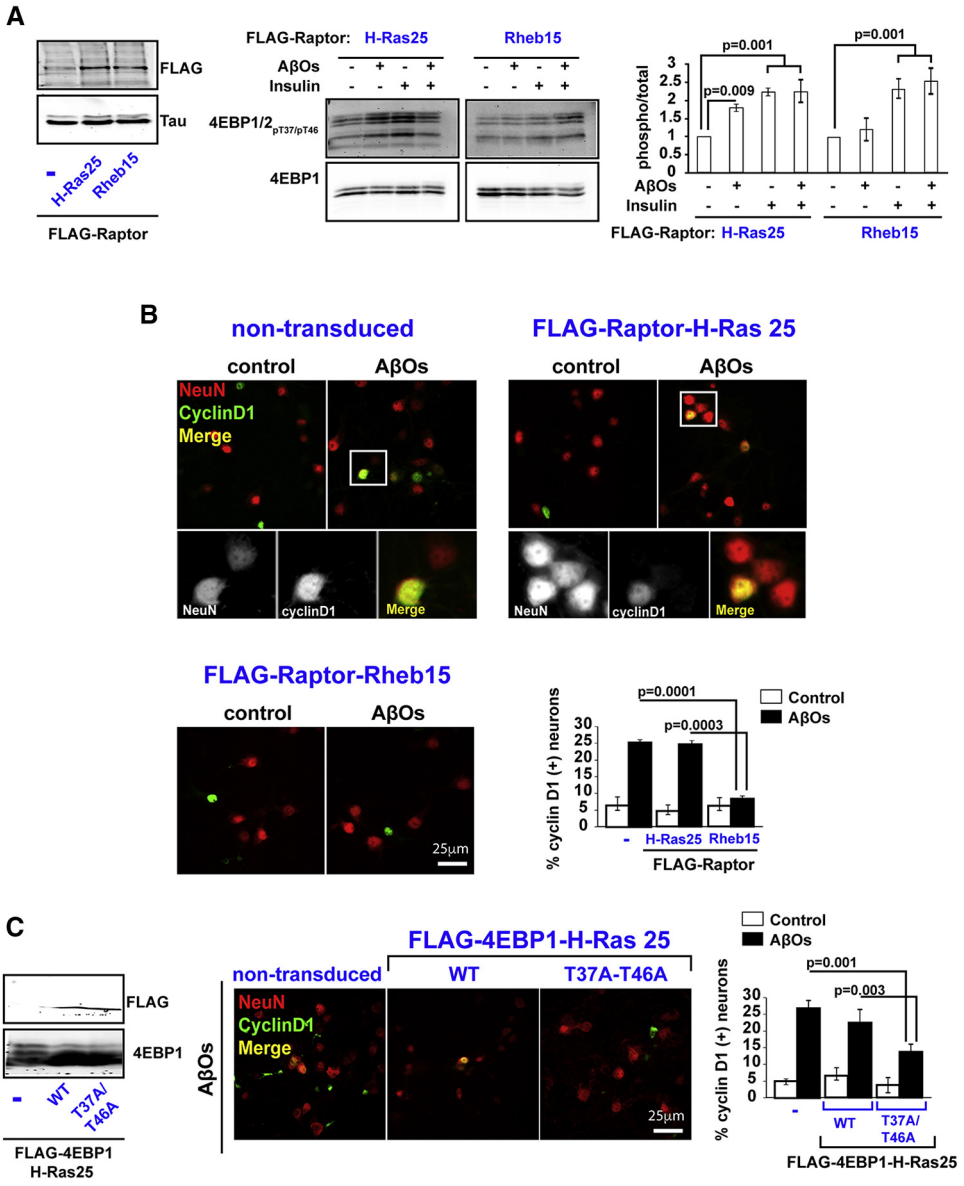

Fig. 2. Amyloid-β oligomers (AβOs) activate mTORC1 at the plasma membrane (PM) but not at lysosomes. Neurons expressing modified mTORC1 subunits targeted to the PM (FLAG-Raptor-H-Ras25) or lysosomes (FLAG-Raptor-Rheb15) were exposed to AβOs or insulin. (A) 4EBP1/2 phosphorylation at T37 and T46 was increased approximately 2-fold by a 30-minute exposure to AβOs, insulin, or a combination of both. (B) Cell cycle reentry (CCR), as monitored by nuclear cyclin D1 localization, was induced by a 24-hour exposure to AβOs when mTORC1 was targeted to the PM but not to lysosomes. (C) AβO-induced CCR, as monitored by nuclear cyclin D1 expression, was supported by overexpressing $4EBP1_{WT}$, but not $4EBP1_{T37A/T46A}$, at the PM. Error bars represent standard error of the mean for three separate experiments.

FLAG-Raptor-Rheb15 was expressed in tau KO neurons, 4EBP1/2 phosphorylation rose slightly after AβO exposure, but the increases were not statistically significant (Supplementary Fig. 3C). These results indicate that the PM-specific activation of mTORC1 by AβOs occurs by a mechanism that requires tau.

4.3. *Rac1 targets mTORC1 to PM lipid rafts for CCR*

Because we previously found that CCR is not blocked by inhibitors of GSK3β [10], which negatively regulates mTORC1 [28], or inhibitors of insulin/IGF-1 receptors, which are upstream of mTORC2 [28], we sought alternative mechanisms linking CCR to mTOR. An shRNA knockdown screen of WT cortical neurons revealed that NCAM, Gαs, and the GTPases, RalA and Rac1, are required for AβO-induced CCR (Fig. 3). NSC23766, which inhibits Rac1 by blocking its interaction with guanine nucleotide exchange factors and thereby maintains Rac1 in the GDP-bound state [30], was also found to inhibit CCR (Supplementary Fig. 4B and C). These results are consistent with prior findings that NCAM is an upstream regulator of fyn and CaMKII [31],

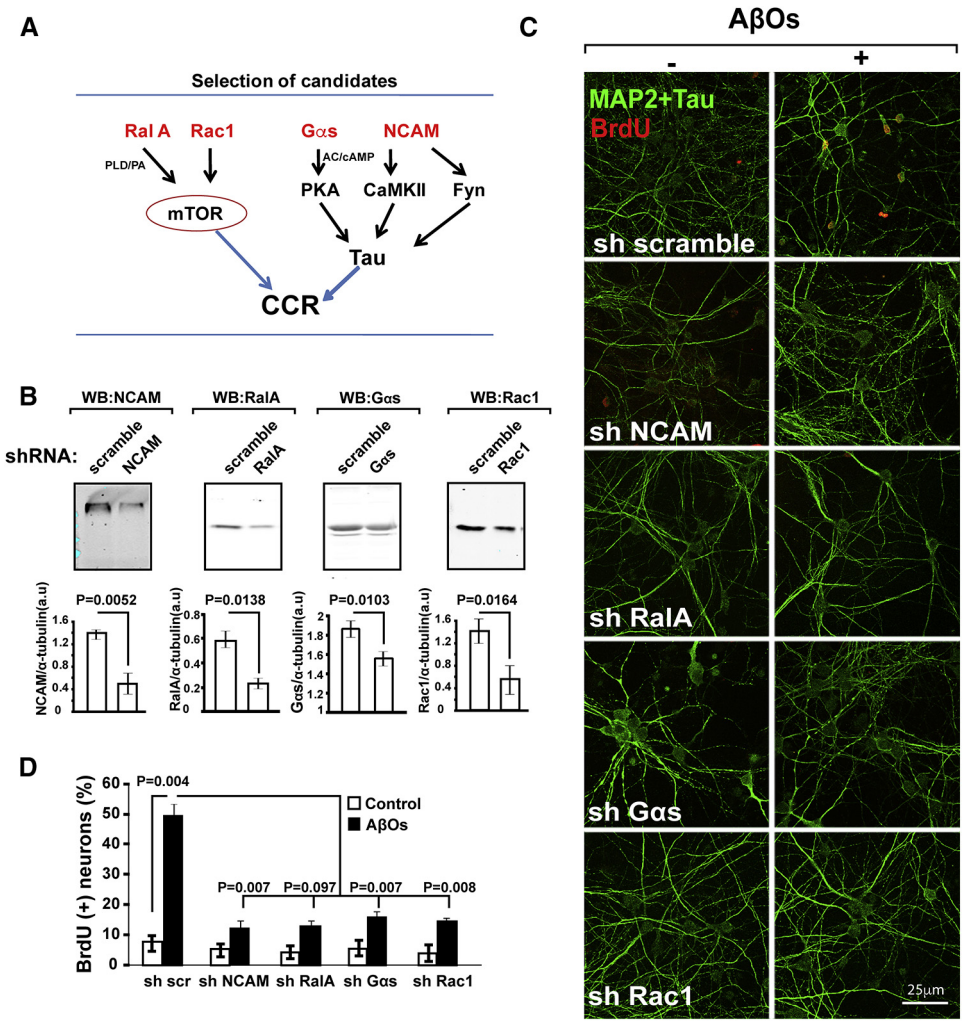

Fig. 3. NCAM, RalA, Gαs, and Rac1 are required for cell cycle reentry (CCR). (A) Selection of candidates based on evidence from other systems. (B) Knockdown efficiency of targeted candidates. (C and D) Amyloid-β oligomer (AβO)–induced CCR, as monitored by nuclear bromodeoxyuridine (BrdU) uptake, is inhibited by knockdown of NCAM, RalA, Gαs, or Rac1. Error bars in (B) and (C) represent standard error of the mean.

that Gαs regulates PKA through its control of adenylate cyclase [32], that RalA is required for activation of phospholipase D, which generates the mTOR activator, phosphatidic acid [33], and that Rac1 targets both mTORC1 and mTORC2 to membranes by directly binding mTOR [14]. The results further indicate that GTP-bound Rac1 is required for CCR, despite the prior finding that Rac1-GTP and Rac1-GDP bind equally well to mTOR [14]. Consistent with these conclusions, we found that shRNA knockdown of Rac1 in WT cortical neurons to ∼40% of normal level caused an ∼60% decrease in 4EBP1/2 phosphorylated by mTORC1 at T37/T46 (Fig. 4A) and ∼70% drops in AβO-induced BrdU uptake and cyclin D1 expression (Fig. 4A and Supplementary Fig. 4A).

Binding of Rac1 to mTOR requires the RKR sequence (amino acids 186–188) located near the C-terminus of Rac1 [14]. To test the importance of the Rac1/mTOR interaction for CCR, we treated primary neurons with the cell-permeable TAT peptide [34] or TAT modified by addition at its C-terminal of a Rac1 peptide containing the WT RKR sequence (TAT-$Rac1_{WT}$) or a sequence in which RKR was mutated to AAA (TAT-$Rac1_{3A}$). Compared with neurons treated with TAT or TAT-$Rac1_{3A}$, neurons treated with TAT-$Rac1_{WT}$ had ∼50% reduction in baseline levels of $S6K_{pT389}$ and $4EBP1/2_{pT37/pT46}$ and an ∼80% reduction in AβO-induced BrdU uptake (Fig. 4B). Because CCR can be blocked by binding of mTOR to the TAT-$Rac1_{WT}$ peptide (Supplementary Fig. 5A), we conclude that Rac1 binding to mTOR is necessary for CCR and is competitively inhibited by TAT-$Rac1_{WT}$.

Membrane binding of Rho GTPases is required for their interaction with downstream effectors and regulators of their catalytic activity. For Rac1, membrane targeting is mediated by a C-terminal, polybasic region, and geranylgeranylation of the cysteine in the adjacent CAAX domain [35]. PM targeting of Rac1 also requires its translocation to lipid rafts [36,37], which are low-density membrane microdomains that integrate cellular signaling process [38].

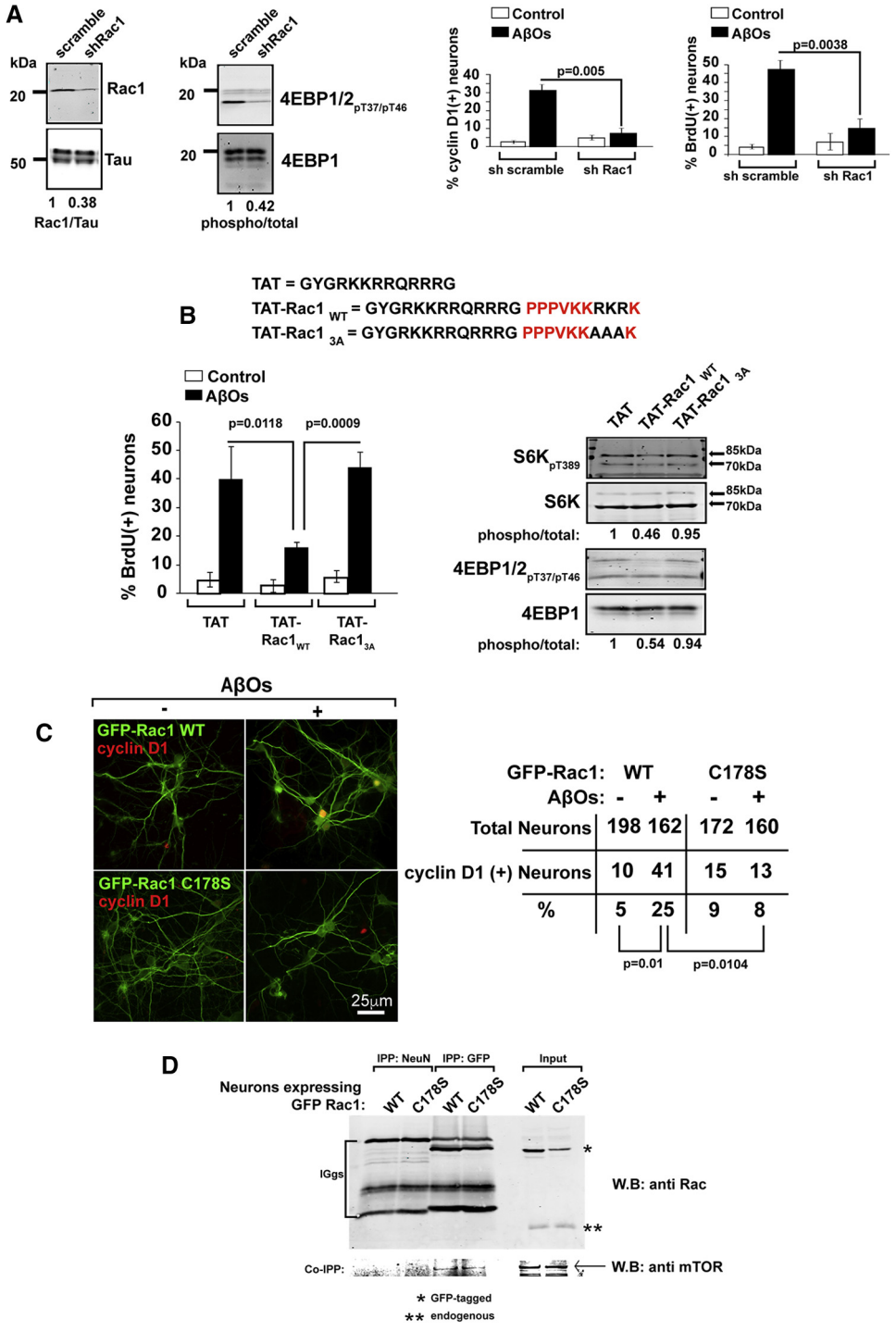

Fig. 4. mTOR targeting to lipid rafts by Rac1 is required for cell cycle reentry (CCR). (A) Rac1 knockdown reduces 4EBP1/2 phosphorylation, nuclear cyclin D1 expression, and bromodeoxyuridine (BrdU) uptake in amyloid-β oligomer (AβO)–treated neurons. (B) TAT-Rac1$_{WT}$ peptide inhibits BrdU uptake, S6K and 4EPB1/2 phosphorylation, and (see Supplementary Fig. 5) Rac1-mTOR interaction in AβO-treated neurons. (C) Expression of GFP-Rac1$_{C178S}$, partitioning of which to lipid rafts is impaired (Supplementary Fig. 5), blocks CCR in AβO-treated neurons. (D) Rac1-mTOR interaction is not dependent on palmitoylation at C178. Error bars in (A) and (B) represent standard error of the mean.

Lipid raft recruitment of Rac1 depends on palmitoylation at C178 and regulates Rac1 activation and function [35]. In WT neurons, partitioning of palmitoylation-deficient GFP-Rac1$_{C178S}$ into lipid rafts is reduced by ~60% compared with GFP-Rac1$_{WT}$ (Supplementary Fig. 5B and C). Moreover, cyclin D1-positive nuclei in neurons expressing GFP-Rac1$_{WT}$ rose approximately 5-fold after AβO exposure but was not increased by expression of

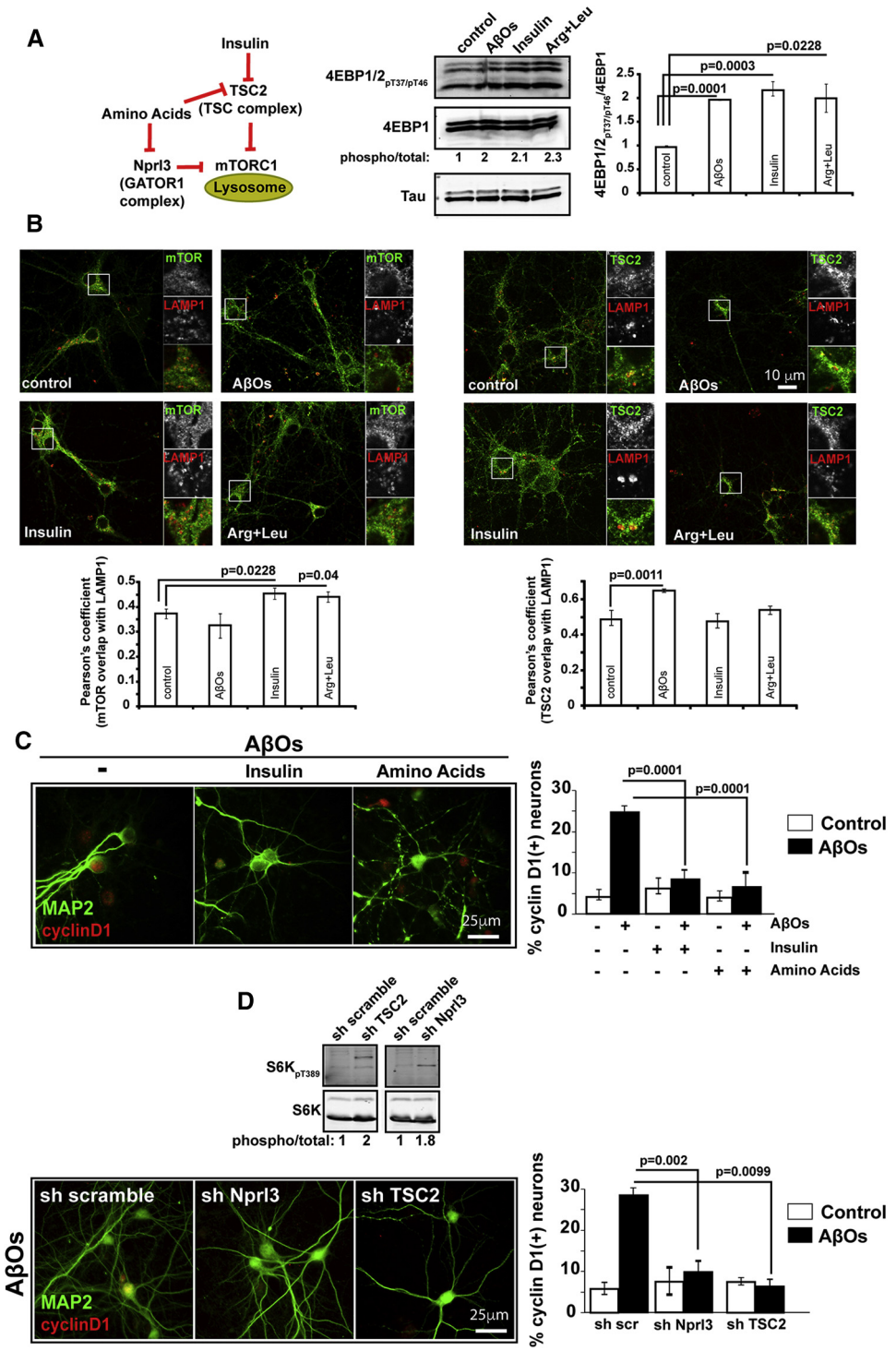

Fig. 5. Insulin or amino acids activate mTORC1 at lysosomes and block amyloid-β oligomer (AβO)–induced cell cycle reentry (CCR). (A) AβOs, insulin, or amino acids (arginine + leucine) stimulate an approximate 2-fold increase in 4EBP1/2 phosphorylation in cortical neurons. (B) Neurons starved of insulin and amino acids for 2 hours were treated with AβOs, insulin, or arginine + leucine for 30 minutes and then were labeled by double immunofluorescence for mTOR and LAMP1 or TSC2 and LAMP1. (C) AβO-induced CCR is blocked by insulin or arginine + leucine. (D) Small hairpin RNA (shRNA) knockdown of Nprl3 or TSC2 blocks AβO-induced CCR. Error bars in all panels represent standard error of the mean.

GFP-Rac1$_{C178S}$ (Fig. 4C). Conversely, AβO-induced, mTORC1-catalyzed phosphorylation of 4EBP1/2 was significantly reduced by expression of GFP-Rac1$_{C178S}$ compared with GFP-Rac1$_{WT}$ (Supplementary Fig. 5D). Finally, immunoprecipitation demonstrated that the palmitoylation-deficiency of GFP-Rac1$_{C178S}$ did not affect

its ability to interact with endogenous mTOR (Fig. 4D). Altogether, these data imply that excessive, AβO-mediated targeting to lipid rafts of Rac1 and mTORC1 to which it is bound triggers downstream signaling required for CCR.

4.4. Lysosomal mTOR activation by insulin or amino acid blocks AβO-induced CCR

Coordinated positioning of mTORC1 and two of its inhibitors on lysosomes regulates mTORC1 activity at that location. One inhibitor, TSC2, dissociates from lysosomes in response to insulin [13] or amino acid [27] stimulation, whereas the other inhibitor, the GATOR1 complex, is inactivated by amino acids [39]. mTORC1 activation at lysosomes is thus coupled to rises in insulin or amino acids (Fig. 5A).

Because AβO-induced activation of mTORC1 occurs at the PM, but not at lysosomes (Fig. 2), we compared the effects of AβOs, insulin, and a mixture of arginine plus leucine on the lysosomal content of mTORC1 and TSC2 in cultured WT cortical neurons. We confirmed by Western blotting of $4EPB1/2_{pT37/pT46}$ that a 30-minute exposure to any of these agents leads to an approximate 2-fold activation of mTORC1 (Fig. 5A). Using immunofluorescence, we also found that insulin or the amino acids causes ∼10% increase in the level of lysosomal mTOR, as judged by its colocalization with the lysosome marker, LAMP1, without altering the level of lysosomal TSC2. In contrast, AβOs did not induce recruitment of mTOR to lysosomes but did increase lysosomal TSC2 by >30% (Fig. 5B). These findings suggest that the failure of AβOs to activate lysosomal mTORC1 (Fig. 2) reflects the lack of resultant mTOR recruitment and gain of TSC2 on lysosomes, neither of which occurs in response to insulin or amino acids. The rise of net 4EBP1/2 phosphorylation induced by AβOs (Fig. 5A) can be explained by activation of mTORC1 at the PM (Fig. 2).

We next determined the effects of insulin and amino acids on CCR. Neither insulin nor arginine plus leucine could induce neuronal CCR, as judged by their failure to cause nuclear accumulation of cyclin D1. Remarkably, however, either of these agents could prevent AβOs from causing CCR (Fig. 5C) without affecting the level of AβO binding to the neuronal surface (Supplementary Fig. 1A and B). We also found that shRNA knockdown of either TSC2 or the GATOR1 complex subunit, Nprl3 [39] (Supplementary Fig. 6), blocked AβO-induced CCR (Fig. 5D). CCR thus results when AβOs stimulate activation of mTORC1 at the PM in the absence of concomitant mTORC1 activation at lysosomes.

4.5. mTOR-dependent tau phosphorylation at S262 is required for CCR

Abnormal tau phosphorylation is a hallmark of AD and non-Alzheimer's tauopathies [40]. Tau is commonly phosphorylated at just a few residues per molecule in normal brain, but AD tau is hyperphosphorylated [40] with ∼45 phosphorylated residues having been detected [41]. Only in a few cases, however, including neuronal CCR, has site-specific phosphorylation been linked to specifically altered tau function [10,42–45]. Because Aβ has been reported to induce tau phosphorylation at S262 by S6K [46], which itself becomes phosphoactivated by mTORC1 [28], we investigated whether tau_{pS262} is required for CCR. First, we determined that Torin1 or shRNA-mediated Rac1 knockdown reduced the level of tau_{pS262} in primary neurons by ∼40% or ∼75%, respectively (Fig. 6A). Next, we found that lentiviral expression in cultured tau KO neurons [47] of human WT tau (2N4R isoform), but not S262A mutated tau, supports AβO-induced CCR (Fig. 6B). Finally, using AD model mice, we observed that pharmacological inhibition of mTORC1 by feeding rapamycin to the 3xTg strain [22] or genetic reduction of mTOR in the Tg2576 strain [23,24] leads to a dramatic decrease in tau_{pS262} (Fig. 6C). Thus, tau phosphorylation at S262 is regulated by mTOR *in vitro* and *in vivo*, probably indirectly through S6K, and is required for CCR (Fig. 6D).

4.6. Coincidence of tau phosphorylation and neuronal CCR in human AD brain

The collective evidence from this study and our prior work on CCR [10] demonstrates that AβO-induced tau phosphorylation at a minimum of four sites—Y18, S262, S409, and S416—is essential for CCR in cultured neurons or mouse models of AD. Here, we show a strong correlation of tau phosphorylation with neuronal CCR in human AD brain tissue. Rapidly fixed brain biopsy samples from 12 normal pressure hydrocephalus patients ranging in age from 61 to 87 (for patient data summaries, see Supplementary Fig. 7A) were analyzed by immunoperoxidase staining for plaques and tangles by a neuropathologist (JM), who concluded that patients 11 and 12 had AD neuropathologic changes according to the established criteria (Supplementary Fig. 7B). Further analysis by double immunofluorescence revealed a strong correspondence in the AD tissues between neuronal CCR, as marked by colocalization of Ki67, a nuclear marker for cells that G1, S, or G2 of the cell cycle, with the neuron-specific nuclear protein, NeuN, and the presence of tau phosphorylated at S262, S409, and S416 (Supplementary Fig. 7C). Although we were not able to detect tau_{pY18} in any of the tissue samples, these results nevertheless reinforce the conclusion that AβO-induced tau phosphorylation at multiple specific sites underlies neuronal CCR in AD.

5. Discussion

5.1. Analysis of results

Despite sustained and heroic efforts on many fronts, the quest to conquer AD has been a frustrating journey that has not yet yielded any disease-modifying therapies. The

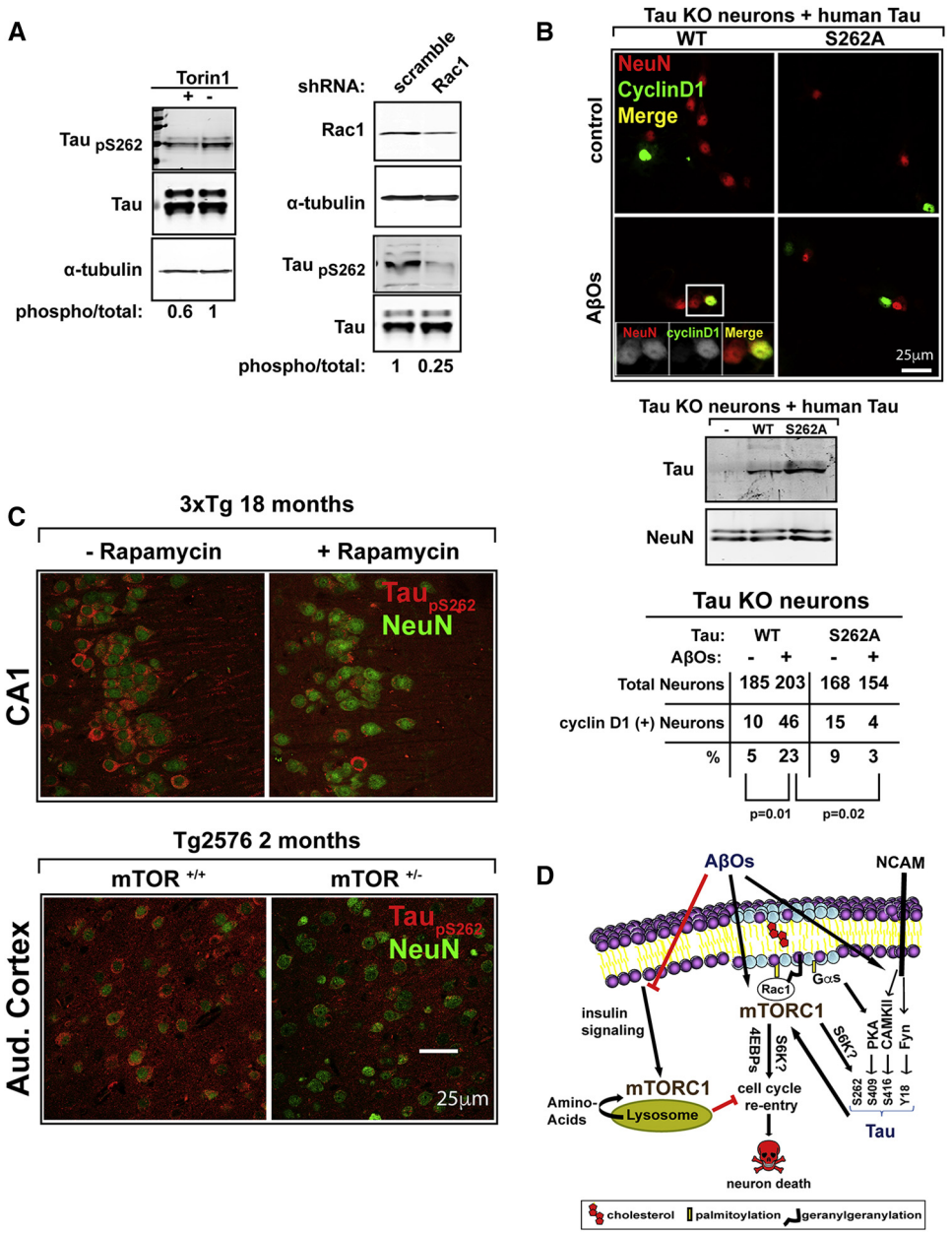

Fig. 6. Cell cycle reentry (CCR) requires mTOR-dependent tau phosphorylation at S262. (A) Baseline level of tau_{pS262} in primary neurons is reduced by Torin1 or Rac1 knockdown. (B) Expression of wild type (WT), but not S262A tau in tau knockout (KO) neurons, restores amyloid-β oligomer (AβO)–induced CCR. (C) Pharmacologic inhibition of mTOR (ad libitum access to rapamycin-laced chow from 2–18 months of age) or mTOR haploinsufficiency reduces tau_{pS262} in Alzheimer's disease (AD) model mice. (D) A model of the neuronal CCR pathway in AD. AβOs initiate two parallel, interconnected pathways that together lead to mTOR dysregulation, which is obligatory for ectopic CCR. One pathway leads from Gαs and NCAM to activation of fyn, protein kinase A (PKA), and calcium/calmodulin-activated kinase II (CaMKII), which then respectively phosphorylate tau at Y18, S409, and S416. The other pathway stimulates translocation of Rac1-mTORC1 complexes to plasma membrane lipid rafts, where mTOR kinase activity is stimulated toward 4EBP1/2 and S6 kinase, and leads to tau phosphorylation at S262. Tau and mTORC1 connect the two pathways.

reasons for this disappointing state of affairs are legitimate topics of debate, but surely include our currently limited understanding at the molecular level of how normal neuronal homeostasis is altered during the earliest stages of AD pathogenesis. Memory and cognitive deficits, the behavioral hallmarks of AD, reflect the dysfunction and loss of synapses among neurons that mediate memory and cognition by the death of those neurons. The study presented here sheds light on how neuron death in AD results from impaired brain insulin signaling [3,4] enabling the apparent reentry of postmitotic neurons into the cell cycle [7–9]. One of the most important features of this

ectopic neuronal CCR is that it occurs independently of amyloid plaque and neurofibrillary tangle formation by a mechanism that is initiated by AβOs, the precursors of the plaques, and requires soluble forms of tau, the building blocks of the tangles. Moreover, cultured neurons express CCR markers within hours of AβO exposure, suggesting that CCR represents a seminal process in AD pathogenesis, and by extension, a possible diagnostic and therapeutic target for AD.

Two key players in the CCR signaling network are mTOR and Rac1. The results presented here demonstrate that both mTORC1 and mTORC2 are required for CCR, that AβOs activate mTORC1 at the PM, but not at lysosomes, that GTP-bound Rac1 in lipid rafts is necessary for the membrane targeting and activation of mTORC1, and that CCR depends on mTORC1-dependent tau phosphorylation at S262. We also show that AβO-induced CCR can be blocked by insulin or amino acids, either of which activates mTORC1 at both the PM and lysosomes. We therefore propose that CCR results from mTOR signaling dysregulation, whereby AβO-induced, tau-dependent activation of mTORC1 occurs at the PM, but is somehow prevented at lysosomes.

Besides initiating this signaling web, AβOs have also been shown to reduce the insulin responsiveness of neurons by activating TNFα/JNK signaling that leads to phosphorylation of IRS-1 at sites that block insulin signaling [48–50]. Microglia play an important role in this process because they secrete TNFα in response to AβOs [51]. AβOs are thus a two-edged sword that both reduce insulin signaling and enable a devastating downstream consequence, CCR, and eventual neuron death. This explains mechanistically why systemic diabetes is a strong AD risk factor and why impaired brain insulin signaling in the absence of systemic diabetes is also associated with AD symptoms [3,4]. Fig. 6C summarizes our current understanding of the CCR signaling network based on the new data presented here, along with relevant, previously published findings [10–12,48–50].

How might mTOR become activated by AβOs? One possibility is by perturbation of membrane microdomains corresponding to lipid rafts. Extracellular AβOs incorporate into neuronal membranes and are gradually recruited to lipid rafts by a fyn-dependent mechanism [52]. At the cell surface, Rac1 is preferentially localized in lipid rafts [36], and as shown here in Supplementary Fig. 5C, a palmitoylation-deficient, GFP-tagged mutant Rac1 that blocks AβO-induced CCR is less efficiently partitioned into lipid rafts than a GFP-tagged WT Rac1 that effectively permits CCR. It is also noteworthy that every one of the protein kinases we have identified as being required for CCR—fyn, PKA, CaMKII, and mTOR (Fig. 6C)—are partially enriched in lipid rafts [52–55], as are NCAM and Gαs [56,57], which we identify here as being upstream of fyn and CaMKII, and PKA, respectively, in the CCR pathway (Figs. 3 and 6C). These collective findings raise the possibility that AβOs perturb lipid raft structure in a manner that causes activation of the kinases, including mTOR, that are required for neuronal CCR.

Although most of the new mTOR data presented here are directed at mTORC1, we did find that inhibition of mTORC2 blocks CCR as effectively as inhibition of mTORC1 (Fig. 1A). This is not surprising in light of the finding that mTORC1 and mTORC2 regulate each other by both positive and negative feedback mechanisms [15,16]. A key feature of this feedback loop is that mTORC1-catalyzed phosphorylation of S6K leads to mTORC2 disassembly and inactivation, which in turn suppresses mTORC1 activity [15]. Perhaps AβOs alter this delicate balance between the two mTOR complexes by somehow bypassing the inhibitory steps of the feedback loop that functionally connect them.

One of the best known effects of mTORC1 activation at lysosomes is suppression of autophagy [58]. Because AβOs activate mTORC1 robustly at the PM, but not at lysosomes (Fig. 2), AβO-induced CCR appears to depend on spatially restricted mTORC1 activation that neither reduces nor enhances autophagic activity. This idea must be considered in the context of in vivo studies of AD model mice, which have demonstrated beneficial effects of autophagy upregulation by rapamycin, namely a reduction of plaques, tangles, and behavioral deficits [18,19,59]. The neutral effects of AβOs on autophagy may therefore be deleterious in two ways. First, by failing to activate lysosomal mTORC1 and thereby suppress autophagy, AβOs evidently dysregulate normal mTOR signaling. Second, by failing to reduce the basal activity of lysosomal mTORC1 and thereby enhance autophagy beyond normal levels, AβOs do not stimulate cells to rid themselves of toxic, misfolded forms of Aβ and tau.

Residing at the center of the CCR story is tau, because without tau AβOs cannot induce CCR either in cultured neurons or in vivo.[10] Importantly, mTOR activation and neuronal CCR have also been shown to result from human tau expression in a *Drosophila* tauopathy model [12]. Although our initial study of CCR led us to conclude that tau phosphorylation at S262 is not necessary to drive neurons out of G0 [10], that conclusion was mistaken and based on assaying tau_{pS262} at a single, 24-hour time point after exposing cultured neurons to AβOs. We now know that AβOs induce transient tau phosphorylation at S262, which returns to baseline level by 24 hours (data not shown). Moreover, because expression of WT, but not S262A tau in tau KO neurons restores their ability to re-enter the cell cycle after AβO exposure (Fig. 6B), tau phosphorylation at S262 and at Y18, S409, and S416 [10] is unequivocally required for CCR. With the exception of pY18, we found a strong correlation between the presence of those phospho-tau epitopes and CCR neurons in human cortical brain biopsy samples from AD patients (Supplementary Fig. S7). The lack of detectable tau_{pY18} in the human tissue could be because of a neuroanatomical limitation. Tau_{pY18} has been detected in

the entorhinal cortex and hippocampus of postmortem AD brain [60], but the rapidly fixed biopsy samples that we examined were limited to superficial cortical areas. Nevertheless, a major challenge for the future will be to identify the molecular mechanisms that phosphorylated tau orchestrates to drive neurons out of G0 and back into the cell cycle.

The pathogenic Aβ-tau connection that underlies neuronal CCR must be considered in the context of the numerous failed efforts to treat AD in humans by reducing Aβ levels and our limited knowledge about tau hyperphosphorylation in most mouse models of AD. The disappointing clinical trials targeting Aβ have been largely directed at mid to late-stage AD patients. The events described here, however, represent AβO-induced, tau-dependent changes that occur in neurons within hours after initial AβO exposure and may not require more sustained AβO insults. Furthermore, none of the tau phosphorylation sites that we identified as being essential for CCR represent canonical AD sites, such as the PHF1 (pS396/pS404), AT100 (pS212/pT214), and AT180 (pT231) phospho-epitopes, that are routinely assayed as indicators of AD tau in AD mouse models and human AD patients. It is therefore noteworthy that we found three of the four tau phosphorylation sites that are necessary for neuronal CCR–pS262, pS409, and pS416—to be increased in human AD brain (Supplementary Fig. 6).

5.2. Clinical implications

How might the new results presented here affect the clinical management of AD? Let us consider diagnosis first. Analysis of cerebrospinal fluid (CSF) as a possible source of AD biomarkers is a promising area of investigation, as a combination of $A\beta_{x-42}$ and tau_{pT181} in CSF has already been promoted as a tool that can accurately diagnose AD ~5 years before clinical symptoms are evident [61]. As encouraging as these results are, perhaps earlier accurate diagnosis can be achieved by assaying CSF for other potential AD biomarkers either individually or in combination, such as those described here and in our previous work on CCR [10]. Examples of such biomarkers include tau phosphorylated at sites we have identified as being required for CCR (Y18, S262, S409, and S416) and mTOR substrate proteins whose phosphorylation at specific sites are indicative of abnormally high mTOR activity in brain (4EBP1/$2_{pT37/pT46}$ and $S6K_{pT389}$).

In terms of potential therapies, the kinases that control tau phosphorylation at sites required for CCR, including mTOR, fyn, PKA, and CaMKII, represent possible targets. Because all those kinases are involved in regulating a variety of cellular process in brain and other tissues, however, the risk of adverse side effects caused by targeting them with drugs is substantial. A noteworthy counterpoint to that concern is the successful use of rapamycin to reduce the histopathology and behavioral decline in the 3xTg strain of AD model mice [18]. Rapamycin is used in humans to treat a few types of cancer, but its modest efficacy and side effects have limited the drug's utility [62]. Perhaps one or more structurally and pharmacologically related "rapalogs" could overcome these deficiencies of rapamycin for treating humans with AD.

One protein that stands out from the crowd as an attractive target for AD therapy is tau. Because tau expression is nearly confined to neurons, any drugs that target tau with high specificity are unlikely to cause complications outside of the brain, with the possible exception of peripheral nerve. In a plaque-bearing AD mouse model, elimination of one tau gene has been shown to relieve learning and memory deficits [63], raising the possibility that reduction of tau, short of its elimination entirely, would have substantial therapeutic value in humans. Tau reduction could be accomplished in principle by antisense nucleotide therapy, provided reagents that effectively cross the brain-blood barrier can be developed. An alternative approach directed at tau could be to use passive or active immunization to deplete toxic forms of tau from brain. Finally, our finding that insulin blocks CCR opens one more possible therapeutic avenue. Unfortunately, the reduced insulin signaling of AD brain [3,4] precludes the simple administration of insulin as a likely productive strategy for AD treatment. Nevertheless, because the insulin effect on CCR involves its ability to activate lysosomal mTORC1 (Fig. 5), the development of an insulin-independent method for activating lysosomal mTORC1 might reduce neuronal CCR and downstream neuron death to benign levels.

Acknowledgments

This work was supported by the Owens Family Foundation (GSB); National Institutes of Health/National Institute of General Medical Science training grant T32 GM008136, which funded part of ES's PhD training; NIH predoctoral fellowship F31 NS092444 to SK; the University of Virginia President's Fund for Excellence (GSB); Webb and Tate Wilson (GSB); The Virginia Chapter of the Lady's Auxiliary of the Fraternal Order of Eagles (GSB); National Institutes of Health/National Institute on Aging grant R01 AG037637 (SO); the Cure Alzheimer's Fund (GSB); and Alzheimer's Association Zenith Fellowship ZEN-16-363266 (GSB). We also thank Lauren Saunders and Lindsay Roy for technical support; Drs John Lazo and Elizabeth Sharlow for supplying Torin1 and their scientific and editorial suggestions; Drs Charles Glabe and Peter Davies and the late Dr Lester (Skip) Binder for gifts of antibodies; and Drs Martin Schwartz, Konstadinos Moissoglu, Miguel del Pozo, and Alejandra Alonso for gifts of complementary DNA expression vectors.

Supplementary data

Supplementary data related to this article can be found at http://dx.doi.org/10.1016/j.jalz.2016.08.015.

RESEARCH IN CONTEXT

1. Systematic review: Cell cycle reentry (CCR), the reentry of postmitotic neurons into the cell cycle, is a prelude to neuron death that occurs in Alzheimer's disease (AD), and along with synaptic dysfunction, accounts for the learning and memory deficits associated with the disorder. This study was initiated to unravel the pathogenic signaling network that causes CCR, and by extension, to reveal potential new diagnostic and therapeutic targets for AD.
2. Interpretation: This study indicates that the previously described ability of amyloid-β oligomers (AβOs) to impair neuronal insulin signaling unleashes their toxic potential to cause tau-dependent CCR. This is because CCR depends on AβOs activating mTORC1 at the plasma membrane, but not at lysosomes, where mTORC1 activation by insulin blocks CCR.
3. Future directions: At a mechanistic level, defining biochemical steps in the CCR signaling network that require tau is a major goal. At a translational level, leveraging our findings to improve AD diagnostics and therapeutics is the main objective.

References

[1] Huang Y, Mucke L. Alzheimer mechanisms and therapeutic strategies. Cell 2012;148:1204–22.
[2] Bloom GS. Amyloid-beta and tau: the trigger and bullet in Alzheimer disease pathogenesis. JAMA Neurol 2014;71:505–8.
[3] de la Monte SM. Type 3 diabetes is sporadic Alzheimer's disease: mini-review. Eur Neuropsychopharmacol 2014;24:1954–60.
[4] Steen E, Terry BM, Rivera EJ, Cannon JL, Neely TR, Tavares R, et al. Impaired insulin and insulin-like growth factor expression and signaling mechanisms in Alzheimer's disease—is this type 3 diabetes? J Alzheimers Dis 2005;7:63–80.
[5] West MJ, Coleman PD, Flood DG, Troncoso JC. Differences in the pattern of hippocampal neuronal loss in normal ageing and Alzheimer's disease. Lancet 1994;344:769–72.
[6] Bussiere T, Giannakopoulos P, Bouras C, Perl DP, Morrison JH, Hof PR. Progressive degeneration of nonphosphorylated neurofilament protein-enriched pyramidal neurons predicts cognitive impairment in Alzheimer's disease: stereologic analysis of prefrontal cortex area 9. J Comp Neurol 2003;463:281–302.
[7] Arendt T, Bruckner MK, Mosch B, Losche A. Selective cell death of hyperploid neurons in Alzheimer's disease. Am J Pathol 2010; 177:15–20.
[8] Herrup K, Yang Y. Cell cycle regulation in the postmitotic neuron: oxymoron or new biology? Nat Rev Neurosci 2007;8:368–78.
[9] Yang Y, Mufson EJ, Herrup K. Neuronal cell death is preceded by cell cycle events at all stages of Alzheimer's disease. J Neurosci 2003; 23:2557–63.
[10] Seward ME, Swanson E, Norambuena A, Reimann A, Cochran JN, Li R, et al. Amyloid-beta signals through tau to drive ectopic neuronal cell cycle re-entry in Alzheimer's disease. J Cell Sci 2013; 126:1278–86.
[11] Varvel NH, Bhaskar K, Patil AR, Pimplikar SW, Herrup K, Lamb BT. Abeta oligomers induce neuronal cell cycle events in Alzheimer's disease. J Neurosci 2008;28:10786–93.
[12] Khurana V, Lu Y, Steinhilb ML, Oldham S, Shulman JM, Feany MB. TOR-mediated cell-cycle activation causes neurodegeneration in a Drosophila tauopathy model. Curr Biol 2006;16:230–41.
[13] Menon S, Dibble CC, Talbott G, Hoxhaj G, Valvezan AJ, Takahashi H, et al. Spatial control of the TSC complex integrates insulin and nutrient regulation of mTORC1 at the lysosome. Cell 2014;156:771–85.
[14] Saci A, Cantley LC, Carpenter CL. Rac1 regulates the activity of mTORC1 and mTORC2 and controls cellular size. Mol Cell 2011; 42:50–61.
[15] Liu P, Gan W, Inuzuka H, Lazorchak AS, Gao D, Arojo O, et al. Sin1 phosphorylation impairs mTORC2 complex integrity and inhibits downstream Akt signalling to suppress tumorigenesis. Nat Cell Biol 2013;15:1340–50.
[16] Xie J, Proud CG. Crosstalk between mTOR complexes. Nat Cell Biol 2013;15:1263–5.
[17] Oddo S. The role of mTOR signaling in Alzheimer disease. Front Biosci 2012;4:941–52.
[18] Caccamo A, Magri A, Medina DX, Wisely EV, Lopez-Aranda MF, Silva AJ, et al. mTOR regulates tau phosphorylation and degradation: implications for Alzheimer's disease and other tauopathies. Aging Cell 2013;12:370–80.
[19] Caccamo A, Majumder S, Richardson A, Strong R, Oddo S. Molecular interplay between mammalian target of rapamycin (mTOR), amyloid-beta, and tau: effects on cognitive impairments. J Biol Chem 2010; 285:13107–20.
[20] Dawson HN, Ferreira A, Eyster MV, Ghoshal N, Binder LI, Vitek MP. Inhibition of neuronal maturation in primary hippocampal neurons from tau deficient mice. J Cell Sci 2001;114:1179–87.
[21] Dunn KW, Kamocka MM, McDonald JH. A practical guide to evaluating colocalization in biological microscopy. Am J Physiol Cell Physiol 2011;300:C723–42.
[22] Oddo S, Caccamo A, Shepherd JD, Murphy MP, Golde TE, Kayed R, et al. Triple-transgenic model of Alzheimer's disease with plaques and tangles: intracellular Aß and synaptic dysfunction. Neuron 2003;39:409–21.
[23] Hsiao K, Chapman P, Nilsen S, Eckman C, Harigaya Y, Younkin S, et al. Correlative memory deficits, Aß elevation, and amyloid plaques in transgenic mice. Science 1996;274:99–102.
[24] Caccamo A, De Pinto V, Messina A, Branca C, Oddo S. Genetic reduction of mammalian target of rapamycin ameliorates Alzheimer's disease-like cognitive and pathological deficits by restoring hippocampal gene expression signature. J Neurosci 2014;34:7988–98.
[25] Ma XM, Blenis J. Molecular mechanisms of mTOR-mediated translational control. Nat Rev Mol Cell Biol 2009;10:307–18.
[26] Gerdes J, Schwab U, Lemke H, Stein H. Production of a mouse monoclonal antibody reactive with a human nuclear antigen associated with cell proliferation. Int J Cancer 1983;31:13–20.
[27] Demetriades C, Doumpas N, Teleman AA. Regulation of TORC1 in response to amino acid starvation via lysosomal recruitment of TSC2. Cell 2014;156:786–99.
[28] Zoncu R, Efeyan A, Sabatini DM. mTOR: from growth signal integration to cancer, diabetes and ageing. Nat Rev Mol Cell Biol 2011; 12:21–35.
[29] Sancak Y, Bar-Peled L, Zoncu R, Markhard AL, Nada S, Sabatini DM. Ragulator-Rag complex targets mTORC1 to the lysosomal surface and is necessary for its activation by amino acids. Cell 2010;141:290–303.
[30] Gao Y, Dickerson JB, Guo F, Zheng J, Zheng Y. Rational design and characterization of a Rac GTPase-specific small molecule inhibitor. Proc Natl Acad Sci U S A 2004;101:7618–23.
[31] Bodrikov V, Sytnyk V, Leshchyns'ka I, den Hertog J, Schachner M. NCAM induces CaMKIIalpha-mediated RPTPalpha phosphorylation to enhance its catalytic activity and neurite outgrowth. J Cell Biol 2008;182:1185–200.

[32] Northup JK, Sternweis PC, Smigel MD, Schleifer LS, Ross EM, Gilman AG. Purification of the regulatory component of adenylate cyclase. Proc Natl Acad Sci U S A 1980;77:6516–20.
[33] Toschi A, Lee E, Xu L, Garcia A, Gadir N, Foster DA. Regulation of mTORC1 and mTORC2 complex assembly by phosphatidic acid: competition with rapamycin. Mol Cell Biol 2009;29:1411–20.
[34] Green M, Loewenstein PM. Autonomous functional domains of chemically synthesized human immunodeficiency virus tat trans-activator protein. Cell 1988;55:1179–88.
[35] Navarro-Lerida I, Sanchez-Perales S, Calvo M, Rentero C, Zheng Y, Enrich C, et al. A palmitoylation switch mechanism regulates Rac1 function and membrane organization. EMBO J 2012;31:534–51.
[36] del Pozo MA, Alderson NB, Kiosses WB, Chiang HH, Anderson RG, Schwartz MA. Integrins regulate Rac targeting by internalization of membrane domains. Science 2004;303:839–42.
[37] Moissoglu K, Kiessling V, Wan C, Hoffman BD, Norambuena A, Tamm LK, et al. Regulation of Rac1 translocation and activation by membrane domains and their boundaries. J Cell Sci 2014; 127:2565–76.
[38] Lingwood D, Simons K. Lipid rafts as a membrane-organizing principle. Science 2010;327:46–50.
[39] Bar-Peled L, Chantranupong L, Cherniack AD, Chen WW, Ottina KA, Grabiner BC, et al. A tumor suppressor complex with GAP activity for the Rag GTPases that signal amino acid sufficiency to mTORC1. Science 2013;340:1100–6.
[40] Grundke-Iqbal I, Iqbal K, Tung YC, Quinlan M, Wisniewski HM, Binder LI. Abnormal phosphorylation of the microtubule-associated protein tau (tau) in Alzheimer cytoskeletal pathology. Proc Natl Acad Sci U S A 1986;83:4913–7.
[41] Noble W, Hanger DP, Miller CC, Lovestone S. The importance of tau phosphorylation for neurodegenerative diseases. Front Neurol 2013; 4:83.
[42] Alonso AD, Di Clerico J, Li B, Corbo CP, Alaniz ME, Grundke-Iqbal I, et al. Phosphorylation of tau at Thr212, Thr231, and Ser262 combined causes neurodegeneration. J Biol Chem 2010;285:30851–60.
[43] Biernat J, Gustke N, Drewes G, Mandelkow EM, Mandelkow E. Phosphorylation of ser^{262} strongly reduces binding of tau to microtubules: distinction between PHF-like immunoreactivity and microtubule binding. Neuron 1993;11:153–63.
[44] Fath T, Eidenmuller J, Brandt R. Tau-mediated cytotoxicity in a pseudohyperphosphorylation model of Alzheimer's disease. J Neurosci 2002;22:9733–41.
[45] Gauthier-Kemper A, Weissmann C, Golovyashkina N, Sebo-Lemke Z, Drewes G, Gerke V, et al. The frontotemporal dementia mutation R406W blocks tau's interaction with the membrane in an annexin A2-dependent manner. J Cell Biol 2011;192:647–61.
[46] Pei JJ, Bjorkdahl C, Zhang H, Zhou X, Winblad B. p70 S6 kinase and tau in Alzheimer's disease. J Alzheimers Dis 2008;14:385–92.
[47] Wilcock DM, Lewis MR, Van Nostrand WE, Davis J, Previti ML, Gharkholonarehe N, et al. Progression of amyloid pathology to Alzheimer's disease pathology in an amyloid precursor protein transgenic mouse model by removal of nitric oxide synthase 2. J Neurosci 2008; 28:1537–45.
[48] Bomfim TR, Forny-Germano L, Sathler LB, Brito-Moreira J, Houzel JC, Decker H, et al. An anti-diabetes agent protects the mouse brain from defective insulin signaling caused by Alzheimer's disease-associated Abeta oligomers. J Clin Invest 2012;122:1339–53.
[49] De Felice FG, Lourenco MV, Ferreira ST. How does brain insulin resistance develop in Alzheimer's disease? Alzheimers Dement 2014;10:S26–32.
[50] Talbot K, Wang HY, Kazi H, Han LY, Bakshi KP, Stucky A, et al. Demonstrated brain insulin resistance in Alzheimer's disease patients is associated with IGF-1 resistance, IRS-1 dysregulation, and cognitive decline. J Clin Invest 2012;122:1316–38.
[51] Bhaskar K, Maphis N, Xu G, Varvel NH, Kokiko-Cochran ON, Weick JP, et al. Microglial derived tumor necrosis factor-alpha drives Alzheimer's disease-related neuronal cell cycle events. Neurobiol Dis 2014;62:273–85.
[52] Williamson R, Usardi A, Hanger DP, Anderton BH. Membrane-bound beta-amyloid oligomers are recruited into lipid rafts by a fyn-dependent mechanism. FASEB J 2008;22:1552–9.
[53] Partovian C, Ju R, Zhuang ZW, Martin KA, Simons M. Syndecan-4 regulates subcellular localization of mTOR Complex2 and Akt activation in a PKCalpha-dependent manner in endothelial cells. Mol Cell 2008;32:140–9.
[54] Takemoto-Kimura S, Ageta-Ishihara N, Nonaka M, Adachi-Morishima A, Mano T, Okamura M, et al. Regulation of dendritogenesis via a lipid-raft-associated Ca2+/calmodulin-dependent protein kinase CLICK-III/CaMKIgamma. Neuron 2007;54:755–70.
[55] Vang T, Torgersen KM, Sundvold V, Saxena M, Levy FO, Skalhegg BS, et al. Activation of the COOH-terminal Src kinase (Csk) by cAMP-dependent protein kinase inhibits signaling through the T cell receptor. J Exp Med 2001;193:497–507.
[56] Santuccione A, Sytnyk V, Leshchyns'ka I, Schachner M. Prion protein recruits its neuronal receptor NCAM to lipid rafts to activate p59fyn and to enhance neurite outgrowth. J Cell Biol 2005;169:341–54.
[57] Smart EJ, Ying YS, Mineo C, Anderson RG. A detergent-free method for purifying caveolae membrane from tissue culture cells. Proc Natl Acad Sci U S A 1995;92:10104–8.
[58] Noda T, Ohsumi Y. Tor, a phosphatidylinositol kinase homologue, controls autophagy in yeast. J Biol Chem 1998;273:3963–6.
[59] Majumder S, Richardson A, Strong R, Oddo S. Inducing autophagy by rapamycin before, but not after, the formation of plaques and tangles ameliorates cognitive deficits. PLoS One 2011;6:e25416.
[60] Lee G, Thangavel R, Sharma VM, Litersky JM, Bhaskar K, Fang SM, et al. Phosphorylation of tau by fyn: implications for Alzheimer's disease. J Neurosci 2004;24:2304–12.
[61] De Meyer G, Shapiro F, Vanderstichele H, Vanmechelen E, Engelborghs S, De Deyn PP, et al. Diagnosis-independent Alzheimer disease biomarker signature in cognitively normal elderly people. Arch Neurol 2010;67:949–56.
[62] Li J, Kim SG, Blenis J. Rapamycin: one drug, many effects. Cell Metab 2014;19:373–9.
[63] Roberson ED, Scearce-Levie K, Palop JJ, Yan F, Cheng IH, Wu T, et al. Reducing endogenous tau ameliorates amyloid beta-induced deficits in an Alzheimer's disease mouse model. Science 2007;316:750–4.

SUPPLEMENTAL INFORMATION

Figure S1. AβO-binding to the Neuronal Cell Surface Is Not Affected by Amino Acids or Insulin.

(A) Quantification of AβO binding to primary WT neurons by In-Cell westerns [10]. (B) Analysis of AβO binding by confocal microscopy shows the typical punctate cell surface distribution of AβOs, which colocalize extensively with the neuronal marker NrCAM. (C) Cell surface binding of AβOs, as judged by In-Cell westerns, is not statistically different in neurons cultured for 10 versus 15 days.

Figure S2. The mTOR Inhibitors, Rapamycin or Torin1, Prevent AβO-induced CCR in Primary Cortical Neurons.

(A) Antibodies to BrdU and tau were used for immunofluorescence to mark neurons that had incorporated BrdU into nuclei, and thus had entered S phase. AβO-induced CCR was blocked by rapamycin or Torin1 (B) Quantitation of BrdU-positive neurons treated as in panel A. Error bars represent s.e.m.

Figure S3. Tau Is Required for PM-Specific Activation of mTORC1 by AβOs.

Neurons expressing modified mTORC1 subunits targeted to the PM (FLAG-Raptor-H-Ras25) or lysosomes (FLAG-Raptor-Rheb15) were cultured in the absence or presence of AβOs. (A) Detection of transgene expression monitored by anti-FLAG western blotting. (B) Relative mTORC1 kinase activity stimulated by AβOs in primary WT versus tau KO neurons as measured by 4EBP1/2 phosphorylation. Note that stimulated kinase activity was ~2-fold higher in the WT neurons. (C) mTORC1 kinase activity was potently stimulated AβOs in WT neurons at the PM, but not at all at lysosomes, but was not significantly stimulated at either location in tau KO neurons.

Figure S4. AβO-Induced CCR Depends on Rac1-GTP.

(A) Rac1 knockdown suppresses BrdU uptake in neurons exposed to AβOs for 24 hours. (B and C) Rac1 inhibition of GDP-to-GTP exchange for Rac1 with NSC23766 suppresses nuclear cyclin D1 localization and BrdU uptake in neurons exposed to AβOs. Error bars represent s.e.m.

Figure S5. Palmitoylation-Deficient Rac1 Targets Inefficiently to Lipid Rafts and Inhibits AβO-induced CCR.

(A) The TAT-$Rac1_{WT}$ peptide inhibits Rac1-mTOR interaction in cultured WT neurons. (B) GFP-$Rac1_{WT}$ and palmitoylation deficient GFP-$Rac1_{C178S}$ were expressed at equal levels in cultured WT neurons. (C) The C178S mutation reduces partitioning of Rac1 into low density lipid rafts. (D) GFP-$Rac1_{C178S}$ inhibits phosphorylation of the mTOCR1 substrate, 4EBP1/2, at T37 and T46 in AβO-treated neurons. Error bars represent s.e.m.

Figure S6. Knockdown of Tsc2 and Nprl3 in primary WT neurons.

Transgene expression was monitored by western blotting with anti-Tsc2 or anti-Nprl3. Only the high molecular weight region of the anti-Tsc2 blot is shown; no other bands were seen on the remainder of the blot. The molecular weight of Tsc2 is 200,608, but the protein migrates at ~280,000 on this gel system. The anti-Nprl3 antibody recognizes a prominent band in the molecular weight range of Nprl3 (63,605), but numerous additional bands were non-specifically detected.

Figure S7. Coincidence of CCR and Tau Phosphorylation in Human AD Brain.

Rapidly fixed, superficial cortical human brain biopsy samples were obtained from 12 normal pressure hydrocephalus patients. (A) Patient data summary. Patients 11 and 12 had AD neuropathologic changes according to established criteria. Key: -, undetected or rare; +, present; ++, abundant. (B) Immunoperoxidase staining of sections from the indicated patients using antibodies to tau (Sigma catalog # T5530) and Aβ (Millipore catalog # AB5076). (C) Immunofluorescence localization of plaques; the G1/S/G2 marker, Ki67; and tau phosphorylated at S416, S409 and S262. Arrows indicate plaques and patient # is listed on each micrograph.

Table S1.

Antibodies Used in This Study.

Figure S1
Norambuena, et al.

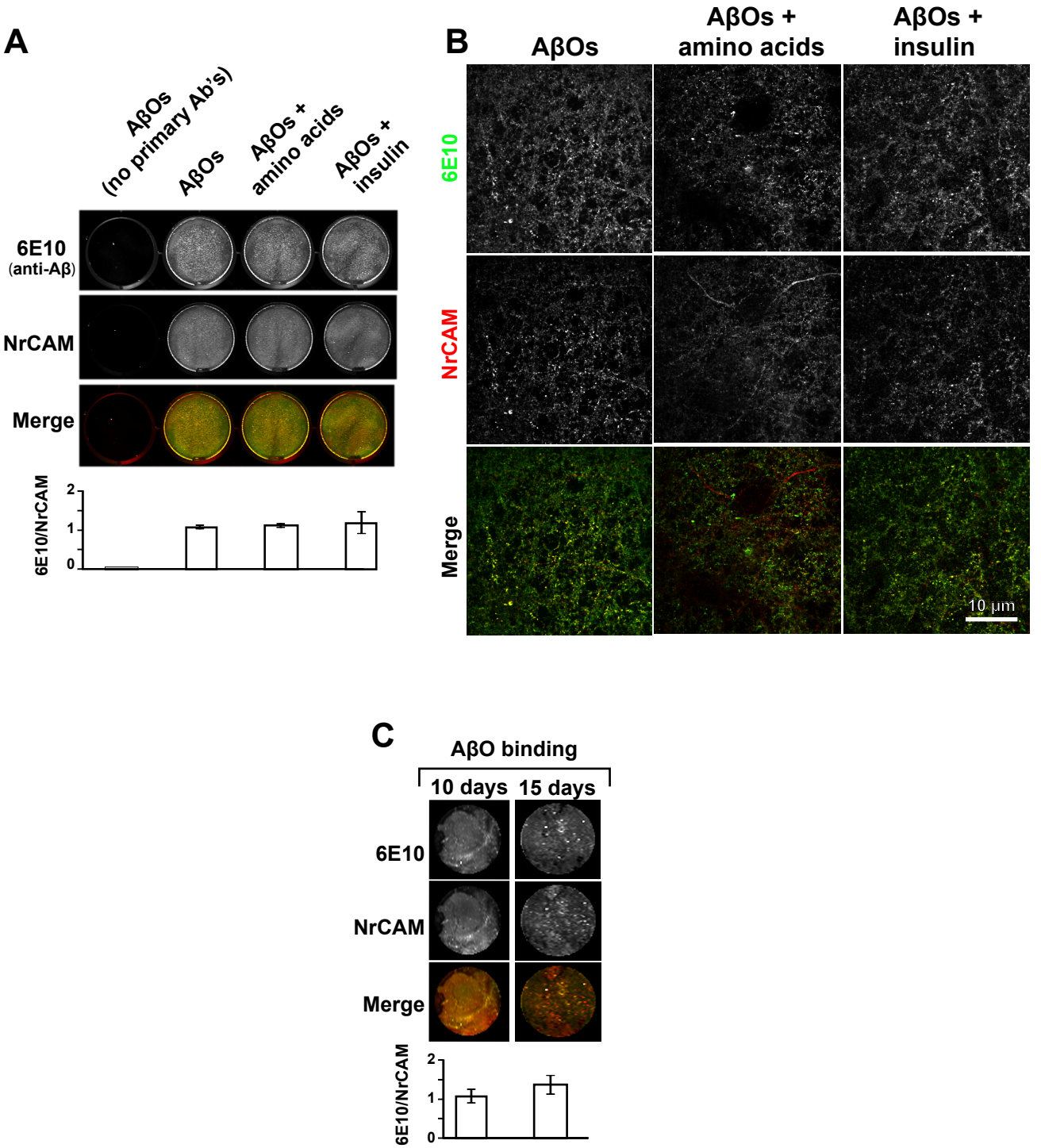

Figure S2
Norambuena, et al.

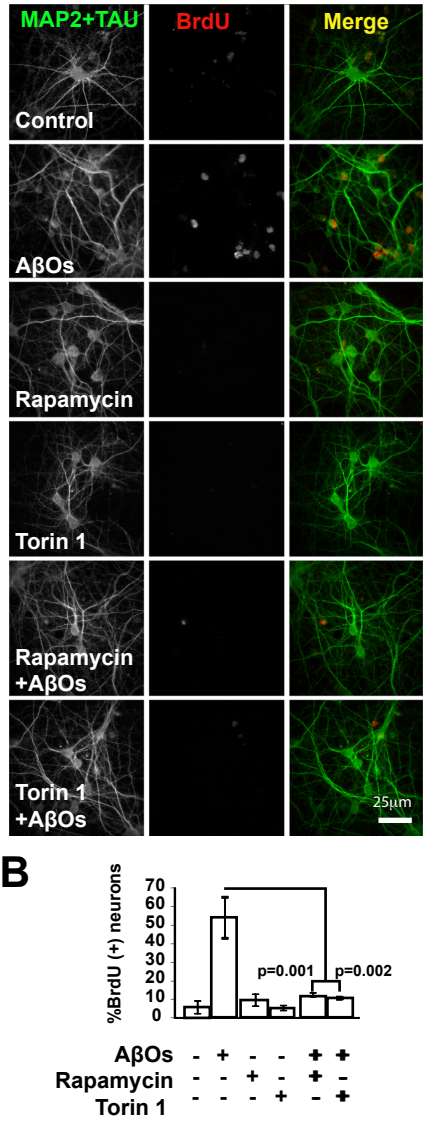

Figure S3
Norambuena, et al.

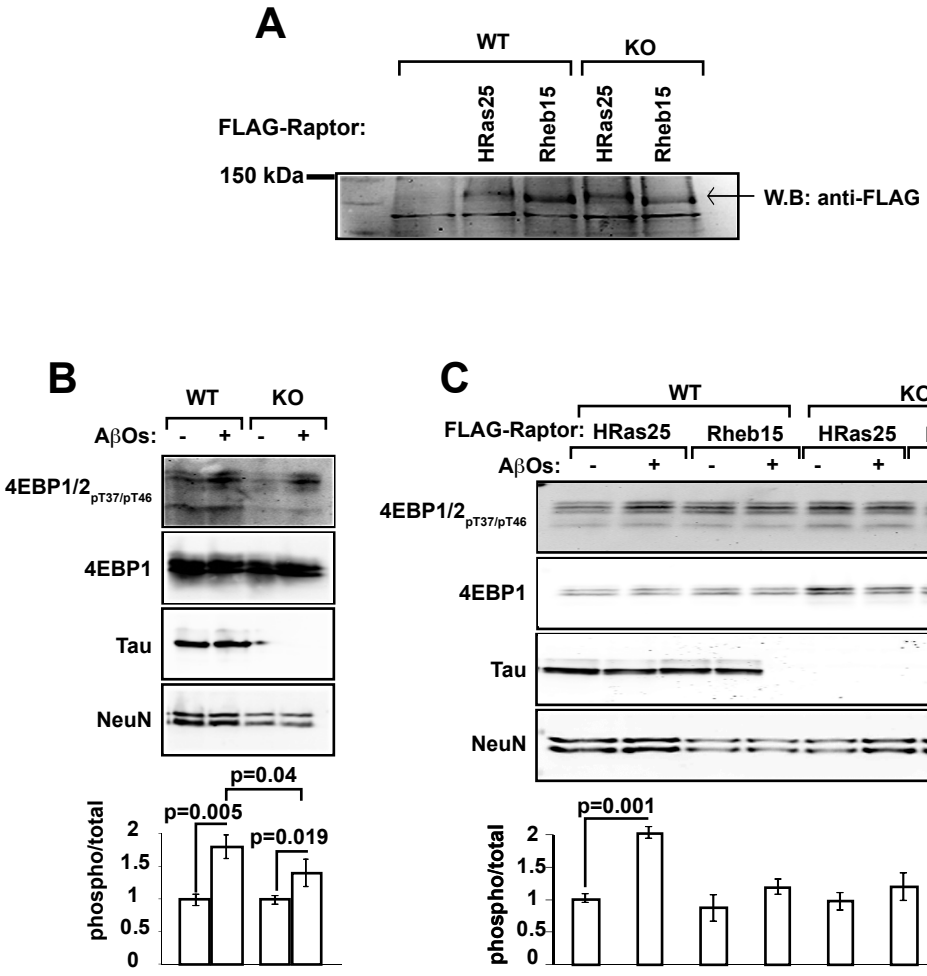

Figure S4
Norambuena, et al.

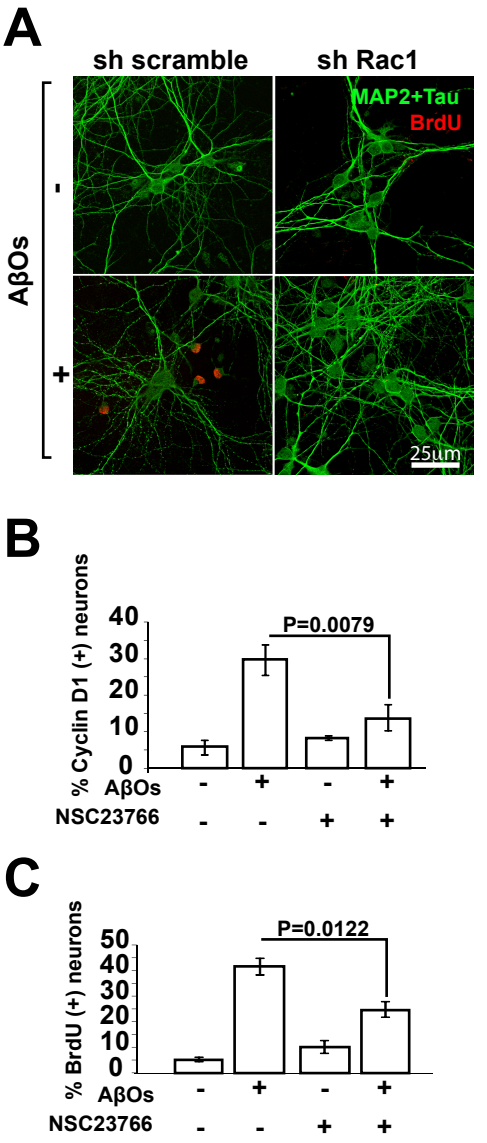

Figure S5
Norambuena, et al.

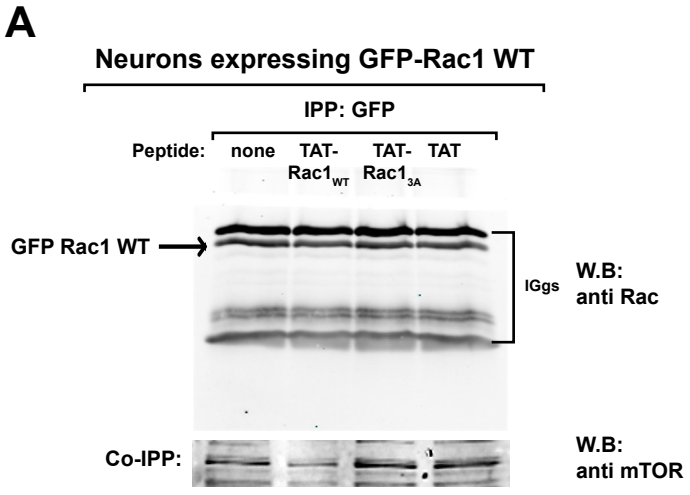

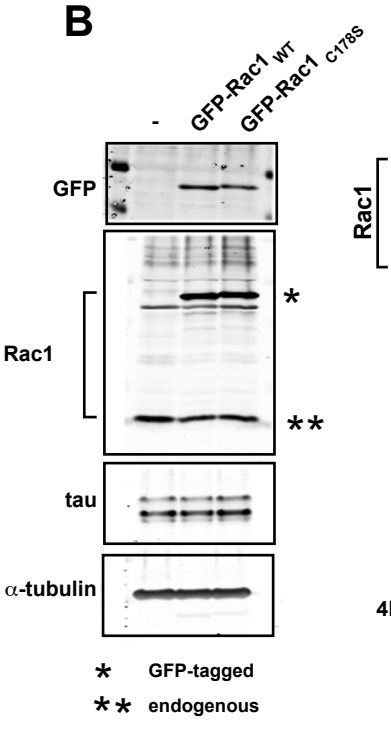

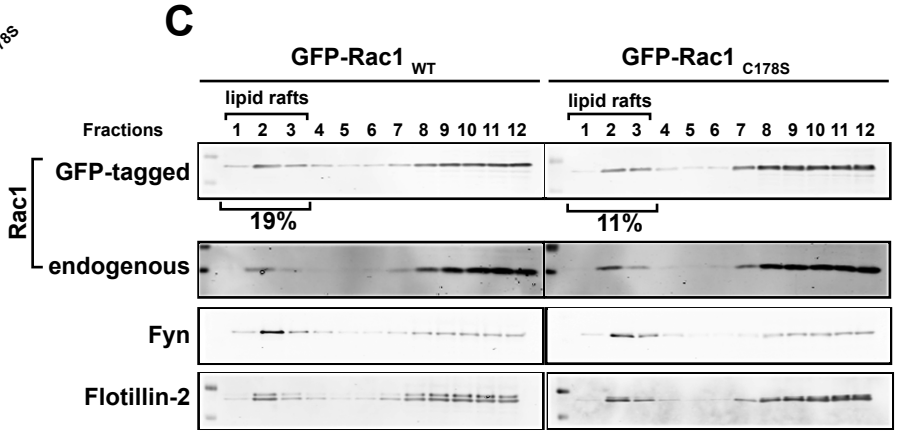

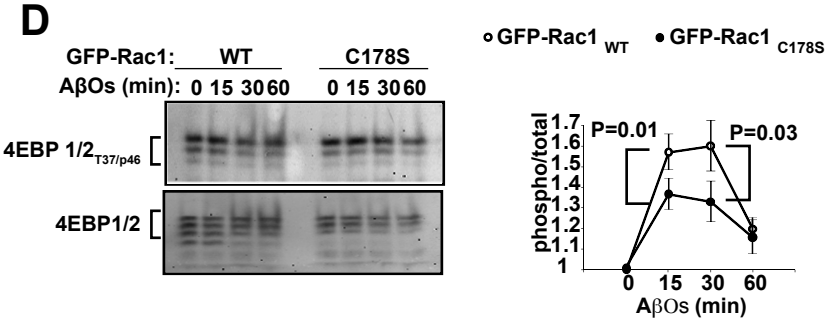

Figure S6
Norambuena, et al.

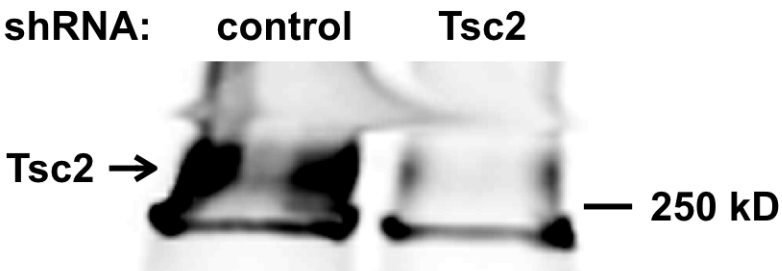

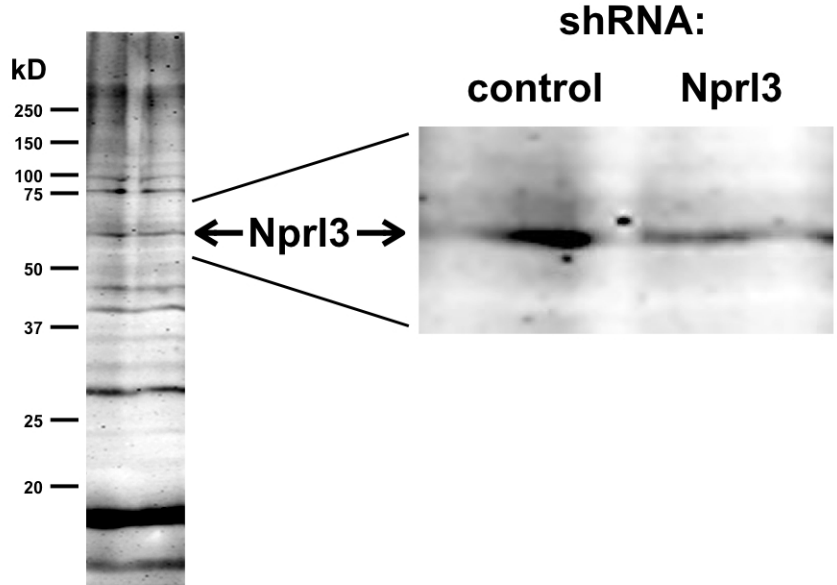

Figure S7
Norambuena, et al.

A

PATIENT	GENDER	AGE	NEUROPIL THREADS	PLAQUES	TANGLES	TAU_{pS262}	TAU_{p409}	TAU_{pS416}	KI67	CYCLIN D1
1	male	79	–	–	–	+	–	–	–	+
2	male	75	–	–	–	+	–	–	+	–
3	male	69	–	–	–	–	–	–	+	–
4	female	75	–	–	–	–	–	–	+	–
6	female	61	–	–	–	+	–	–	+	–
7	male	66	–	–	–	–	–	–	+	undetermined
8	male	67	+	+	+	++	++	++	++	++
9	female	87	–	+	–	+	+	–	+	+
10	male	77	–	–	–	–	–	–	+	+
11	male	72	++	++	++	++	++	++	++	+
12	female	82	++	++	++	++	++	++	++	undetermined

B

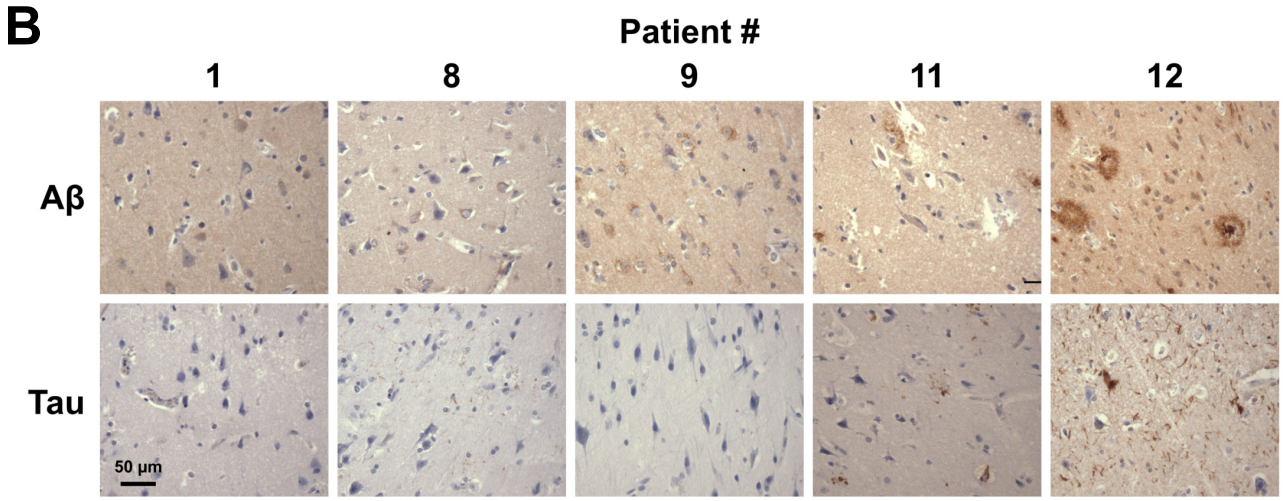

C

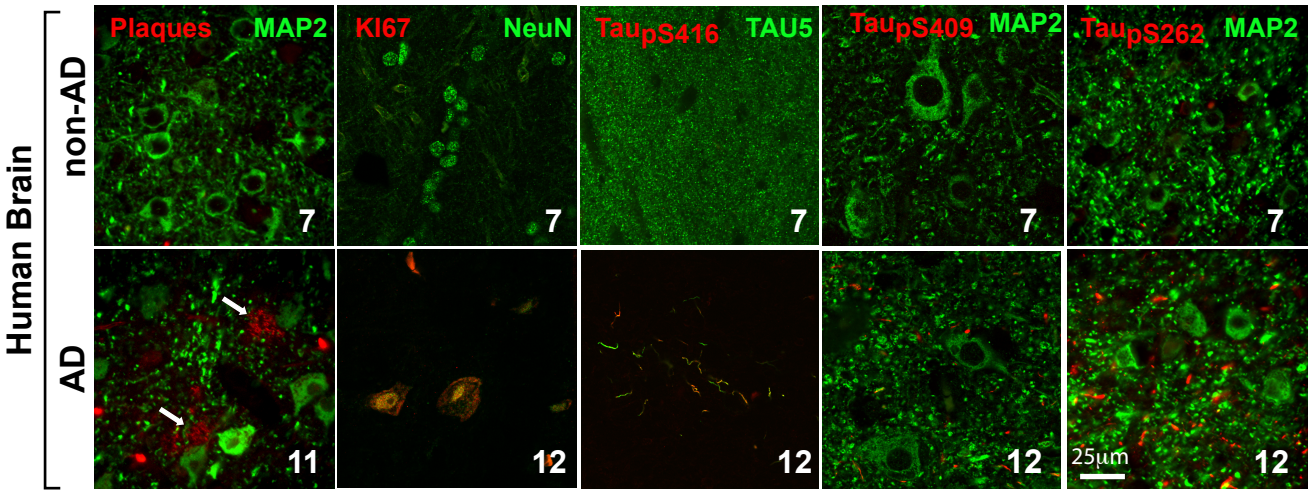

Table S1:
Primary and Secondary antibodies

Antigen	*Host*	*Application*	*Dilution*	*Source/Cat no.*
Aβ (clone M116 Parenchymal amyloid plaques)	Rabbit (monoclonal)	IF	1/100	Dr. Charles Glabe/UC Irvine
Aβ	Mouse	IF	1/100	Millipore/AB5076
Tau (clone 5)	Mouse	IF, WB	1/500-1/5000	LI Binder/ Northwestern U
Tau (clone 2)	Mouse	IF	1/100	SIGMA/T5530
Tau (clone R1)	Rabbit	IF, WB	1/100-1/10000	LI Binder/ Northwestern U
Tau (S409)	Mouse	IF	1/500	Dr. Peter Davies/Feinstein Institute for Medical Research
Tau (S262)	Rabbit	IF, WB	1/100-1/3000	Anaspec/AS-54973
Tau (S416)	Rabbit	IF	1/3000	Antibodies Online,Inc/ABIN361456
Rictor	Rabbit	IF, WB	1/100-1/3000	Cell Signaling Technologies/2114
Raptor	Rabbit	IF, WB	1/100-1/3000	Cell Signaling Technologies/2280
TSC2	Rabbit	IF, WB	1/100-1/3000	Cell Signaling Technologies/D93F12
Akt	Rabbit	WB	1/100-1/3000	Cell Signaling Technologies/9272
Akt (S473)	Rabbit	WB	1/3000	Cell Signaling Technologies/9271
S6K (clone 49D7)	Rabbit	WB	1/5000	Cell Signaling Technologies/2708
S6K (T389)	Rabbit	WB	1/3000	Cell Signaling Technologies/9205
4EBP1	Rabbit	WB	1/5000	Cell Signaling Technologies/55H11
4EBP1/2	Rabbit	WB	1/3000	Cell Signaling Technologies/9459
eIF4E	Rabbit	IF	1/100	Cell Signaling Technologies/2067
fyn	Rabbit	WB	1/3000	Cell Signaling Technologies/4023
RalA	Mouse	WB	1/3000	BD Biosciences/610222
Flotillin-2	Mouse	WB	1/3000	BD Biosciences/610383
Gαs	Rabbit	WB	1/3000	Santa Cruz/SC823
Rac1	Mouse	IF, WB	1/500-1/5000	Upstate/05389
cyclinD1	Rabbit	IF	1/200	Abcam/16663
MAP2	Rabbit	IF	1/200	SIGMA/M3696
α-tubulin	Mouse	WB	1/10000	SIGMA/T6199
NCAM	Mouse	WB	1/3000	DSHB/5B8
LAMP1	Rat	IF	1/250	DSHB/1D4B
Ki67	Rabbit	IF	1/100	Millipore/AB9260
NeuN	Mouse	IF	1/1000	Millipore/MAB377
BrdU	Mouse	IF	1/100	SIGMA/B8434
GFP	Mouse	IF	1/1000	NeuroMab UC Davis/N86/38
6E10	Mouse	IF, In-Cell WB	1/1000	Covance
NrCAM	Rabbit	IF, In-Cell WB	1/1000	Abcam
Flag	Rabbit	WB	1/3000	SIGMA/F7425
AlexaFluor 488	Goat Anti Chicken IgG	IF	1/500	Life technologies/A11039
AlexaFluor 488	Goat Anti Rabbit IgG	IF	1/500	Life technologies/A11008
AlexaFluor 488	Goat Anti Mouse IgG	IF	1/500	Life technologies/A11001
AlexaFluor 594	Goat Anti Rabbit IgG	IF	1/500	Life technologies/A11012
AlexaFluor 594	Goat Anti Mouse IgG	IF	1/500	Life technologies/A11005
AlexaFluor 647	Goat Anti Rat IgG	IF	1/500	Life technologies/A21247
IRDye 800	Goat Anti Mouse IgG	WB, In-Cell WB	1/10000	LI-COR/926-32210
IRDye 680	Goat Anti Rabbit IgG	WB, In-Cell WB	1/10000	LI-COR/936-68171